A review of commercial numerical modelling approaches for axial hydrokinetic turbine wake analysis in channel flow

Niebuhr, C.M.[1,*], Schmidt, S.[2], van Dijk, M.[1], Smith, L.[3] & Neary, V.S.[4]

[1]Department of Civil Engineering, University of Pretoria, Pretoria 0001, South Africa.
[2]Institute of Aerodynamics and Fluid Mechanics, Technical University of Munich, D-85748, Munich, Germany.
[3]Department of Mechanical Engineering, University of Pretoria, Pretoria 0001, South Africa.
[4]Sandia National Laboratories, Albuquerque, NM 87185, USA.

*Corresponding author: Chantel Monica Niebuhr, Email: chantel.niebuhr@up.ac.za

Abstract

Computational fluid dynamics are employed for detailed predictions of hydrokinetic turbine performance and wake modelling. Of these, Reynold-average Navier-Stokes (RANS) models are most widely used due to their ability to resolve power performance and detailed flow features at relatively low computational costs and acceptable accuracy. The limitations of these models are often not well understood when applied to complex turbine and wake dynamics which could lead to potential inaccurate and inappropriate conclusions. This paper focuses on the prediction of the wake generation, dissipation and flow recovery using commercially available modelling software. The approach and findings of previous numerical investigations on this matter is reviewed and compared to experimental measurements reported for a dual-rotor reference turbine. The shortcomings of these models are discussed and appropriate modelling techniques for the preliminary design or analysis of hydrokinetic turbines and inland energy generation schemes are identified. Commercially available RANS models show a good correlation of turbine performance. However, prediction of the wake behaviour is improved by using a virtual disk model with the blade element momentum theory, employing Reynolds's stress closure models. These models allow for modelling the anisotropic conditions in the wake unlike the more popular eddy viscosity models. In addition, simplified rotor geometry models using blade element momentum theory are found to adequately model wake development and dissipation at a modest computational expense. The shortcomings of other approaches in terms of wake dissipation prediction and the effect of boundary and inflow conditions are analysed, emphasizing the importance of correct prescriptions of model parameters.

Keywords

Hydrokinetic, Computational fluid dynamics, Wake-dissipation, In-land hydrokinetic, Axial flow turbines, wake-modelling.

Word count: 9 862

Abbreviations

λ	Tip speed ratio
AD	Actuator disk
ADV	Acoustic Doppler velocimetry
BEM	Blade element momentum
CFD	Computational fluid dynamics
Cp	Calculated power coefficient
D	Diameters
DES	Detached eddy simulation
ECA	Energy capture area
FRG	Full rotor geometry
GCI	Grid convergence index
HAHT	Horizontal axis hydrokinetic turbine
HK	Hydrokinetic
IDDES	Improved delayed- detached eddy simulation

LDV Laser Doppler velocimetry
LES Large eddy simulation
LPS Linear pressure strain
LRR Launder-Reece-Rodi
PIV Particle image velocimetry
RANS Reynolds-averaged Navier-Stokes
RM1 Reference model 1
RSM Reynolds stress model
SST Shear stress transport
TI Turbulence intensity
TKE Turbulent kinetic energy
URANS Unsteady Reynolds-averaged Navier-Stokes
VD Virtual disk

Contents

1 Introduction

1.1 Inland Hydrokinetic Energy

Inland hydrokinetic energy has seen increased research and development activity in the last ten years. This includes studies that assess the resource for regional and national renewable energy portfolios, e.g. [1], studies characterizing the ambient turbulent inflow conditions and wake effects, e.g., [2,3], studies demonstrating hydrokinetic (HK) turbine technologies [4,5] and specific focus on characterization and assessment of the spatiotemporal variation in the current velocity and turbulence acting on the turbine rotor [2].

For inland horizontal axis hydrokinetic turbines (HAHT) schemes, like wind farms, devices are placed in arrays to increase the annual energy production and optimize the techno-economic performance [5]. Within array

schemes, prediction of the upstream wake effects on the ambient inflow conditions is of primary importance[6]. Disregard of these effects can result in reduced efficiencies of downstream turbines [7,8]. and a combined large scale effect of the array on the environment [9,10]. A thorough review of these complex wake dynamics are reported by Fontaine et al. [4].

The current advancements in computational efficiency and capacity incentivise the use of complex CFD models for inland HK turbines modelling to expand on the existing knowledge base. Computational investigations on both performance and wake effects are providing a much clearer picture of the flow-structure interaction and power output of HK installations. The impact environmental effects such as blockage [11], flow speed [12], yawed flow [13] have on turbine performance may be better understood through computational modelling. Additionally the primary wake recovery mechanisms [14] and wake interactions [15] have also been analysed. A more informed understanding of these complex flow effects enables an improvement of the design and installation of HK devices. This also provides more clarity on site selection [16], proper array spacing [17] and other challenges surrounding operations and maintenance.

1.2 Modelling of hydrokinetic devices

Numerical/computational modelling techniques may be used as a tool to assess possible concerns, problem areas and unforeseen hydrodynamic effects in the HK turbine flow field. Laboratory tests are often expensive and prove difficult to accurately scale the flow environment [16]. Inland hydrokinetic turbines or turbine arrays are often placed in constrained flow areas that are only one or two orders of magnitude larger than their energy extraction planes [17], therefore accurate modelling of blockage and free surface effects are important [18].

Uniformity laws and “scales of modelling” are important considerations within computational models. This ensures dependant variables are included and computational resources are focussed on key aspects. For tidal applications scales of hydrodynamic modelling have previously been developed to address the required accuracy at each scale [19]. A similar approach may be applied to inland HK systems. The four primary scales of modelling are represented in Figure 1. Each scale has a focus and may be more specifically defined as:

1] Device scale (blade scale):
   a. Focus on the flow around the turbine blades, lift and drag, performance analysis [4,16,19]
   b. Important to capture the ‘dynamic stall’ due to the massive flow separation [4] to accurately predict turbine performance.
   c. Important to capture effects of blade roughness (fouling), e.g., [4,20]
   d. Important to capture effects of submergence and cavitation[4,13]
   e. Important to capture blade wakes and tip vortices, e.g., [4,16]
   f. Requires highly accurate simulations resolving the large eddies not only in the wake, but also the boundary layer still attached to the blades [21,22].
2] Device scale (rotor scale) flow field analysis:
   a. Analysing the bulk thrust load and wake resulting from specific operating conditions [23].
   b. Effect of local flow conditions e.g. ambient turbulence [24,25]
   c. Prerequisite to determining placement of array schemes.
3] Array scale (channel scale) analysis:
   a. Turbine inter-effect (Interaction of multiple turbines).
   b. Effect of local flow conditions, e.g., ambient turbulence [26]
   c. Simplified techniques such as porous disc method [7] or Blade element momentum theory applied on an actuator disk (BEM-AD) together with Reynolds-averaged Navier-Stokes (RANS) equation models [27,28] or Actuator line Large eddy simulations (LES) [29]
4] Far field flow analysis (full system analysis):
   a. Analysis of far field backwater effects, blockage effects, erosion, sedimentation.
   b. Simplified 1-dimensional or 2-dimensional modelling using simplified numerical or analytical models [30–33]

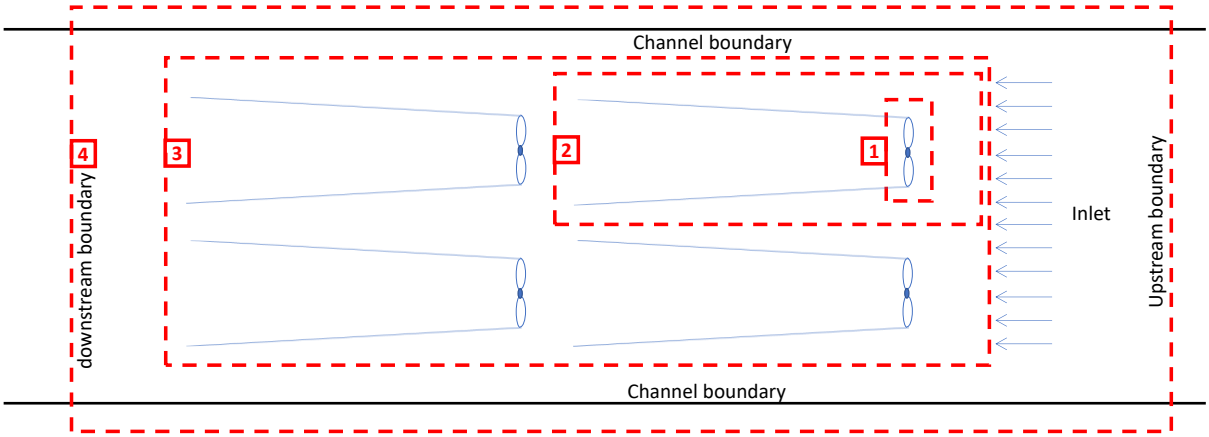

Figure 1: Scales of modelling inland HK schemes

As summarized in [4], numerous physical modelling studies have investigated device scale physics, including wake generation, dissipation and flow recovery downstream of a single turbine, e.g., [15], [21-23]. Similar numerical modelling investigations have been performed [34–38]. Clear guidelines on suitable computational approaches and methods to avoid inaccuracies and errors are lacking. This paper serves to address the limitations of the approaches and methods usually employed in the modelling of specifically the device scale flow field. This is of crucial importance for inland schemes, where spatial constraints are restrictive and optimal spacing is essential to maximize power generation and annual energy production.

1.3 Hydrokinetic wake development for channel flow

Placing a turbine in a moving flow field causes a disturbance in the downstream region. This region is characterized by intense turbulent mixing, helical movements and a complex eddy system referred to as the wake [39].

Understanding wake formation is critical in HK installation and array optimisation. Like wind turbines, water turbine wake dynamics and structures exhibit wake rotation, wake meandering [40], the evolution of the shear layer, significant momentum transport across this shear layer, and dynamic interaction and breakdown of hub, tip and stanchion vortices within and at the interface of the coherent wake structure [4,40]. However, there are clear differences for water turbine wake structures operating in depth-limited boundary layer flows. Including changes in fluids interacting with the bounding surfaces/free surface [36]. Additionally, far wake velocity deficits do not have the symmetric Gaussian profiles typically found downstream of wind turbines in unconfined atmospheric boundary layer flows, and these constraints can strongly affect flow recovery (as proven in previous studies [41,42]).

Figure 2 may be used to describe a turbine wake and propagation thereof. Consider a turbine of area A in channel cross sectional area A_c Consider cross section A_o as the stream tube area in upstream undisturbed flow where the pressure is p_o and flow speed u_o. The stream tube pressure is p_1 just upstream of the turbine and p_2 just downstream (assumed uniform as in the Lanchester-Betz formulation). The stream tube then continues to expand downstream of the turbine before settling to a constant area A_3 with speed u_3. The speed of flow outside the wake is u_4 and pressure p_4. As indicated on the sketch as A_c approaches infinity $p_4=p_0$ and $u_4=u_o$ (depending on the blockage ratio). The flow further downstream allows lateral mixing which results in a change of pressure to p_5 which varies from p_0 [43]

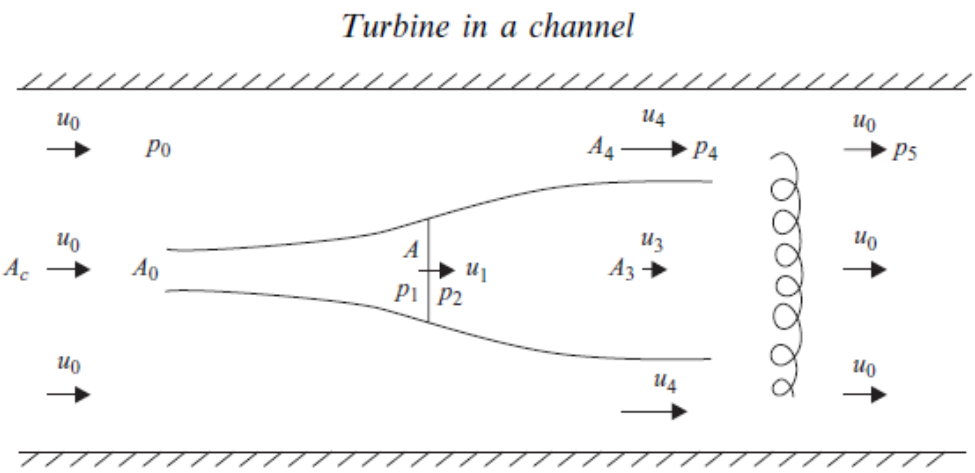

Figure 2: Definition for single turbine in a channel [43]

The energy extraction is obtained through applying the momentum and Bernoulli equations to the flow field in Figure 2 [43]. For a channel in an infinitely large domain, the maximum efficiency has been found to be around 0.59 (however the effect of confinement on this efficiency has not been investigated). Immediately downstream of the turbine the wake physics is complex, and is influenced by the bypass flow, induced flow rotor and specific tip vortex interaction with the supporting structure [44]. Further downstream the wake starts mixing with the bypass flow and causes wake expansion inducing velocity recovery occurring over a long distance downstream.

The typical wake structure of a HK device can be split into two zones with different primary behaviour, namely the near and far wake. The end of the near wake may be categorized as the point with highest velocity deficit as indicated in Figure 3. Further downstream the wake starts mixing with the bypass flow, resulting in wake expansion and velocity recovery. This wake region is characterized by intense turbulent mixing, helical movements, and a complex eddy system. This may be attributed to two phenomena, the instability of boundary layers on the blades due to the adverse pressure gradient along the rotor plane and a spiral vortex structure which is shed outwards from the blade tip and rotor root. The latter produces large eddies in the flow which last a long distance downstream (far wake region) [34].

Multiple physical processes exist in the flow affecting the performance and wake of a HK device. These include the onset shear and turbulence, interaction with the retaining structure, tip vortices and wake rotation (as indicated in Figure 3). The near wake is characterised and affected by the turbine geometry, whilst the far wake, less so [32]. To allow accurate prediction of the near and far wake numerical models may be used, and care should be taken to ensure all factors affecting the wake as well as the complex flow in the wake itself are captured.

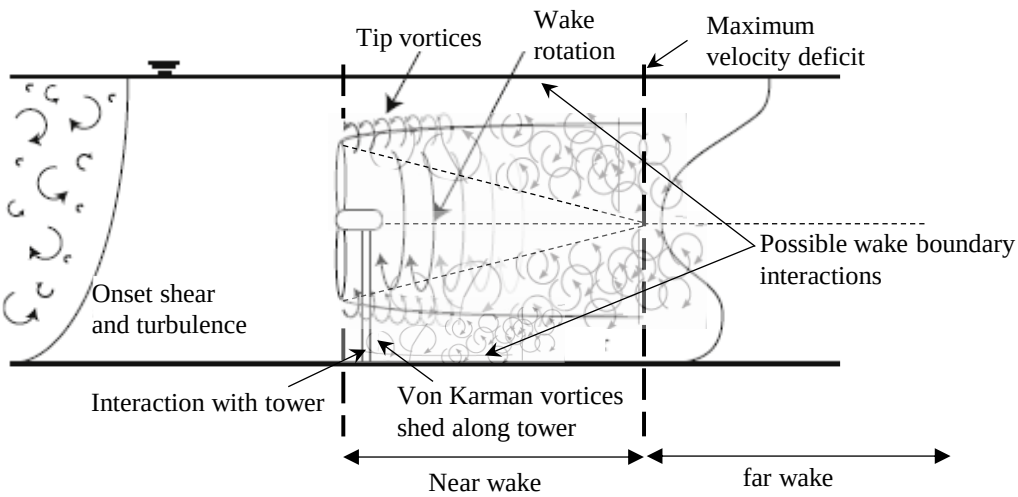

Figure 3: Schematic of flow affecting the loading and wake of a HK device (adapted from [44,45]**)**

Results from previous studies on HK turbines placed in channels with similar Reynolds numbers to typical inland installation may be used as an indication of the development and length of a typical HAHT wake. These studies have indicated wake velocity deficits exceeding 10-20 rotor diameters (D) downstream [25,26]. Chamorro et al. [40] observed a wake propagating further than 15 D downstream. Bahaj et al [36] presented wake centreline measurements indicating a velocity deficit for distances exceeding 20 D. A study by Edmunds et al. [46] drew a comparison of experimental and numerical results at a tip-speed ratio (TSR) of 3.7 where the wake spread and reduced from a 22% velocity deficit at 1.2 D to a 12% deficit at 10 D. In one of the few documented far field experimental studies completed on an three-bladed HAHT, the far field wake measurements indicated a velocity deficit propagating further than 35 D downstream [8]. With wake measurements indicating an 80% recovery at around 10 D downstream. Studies showed similar trends where the velocity deficit decays exponentially starting at 3 D downstream and reaches approximately 80% recovery between 9-10 D before maintaining an almost constant value to 35 D downstream (Only indicated in [8]). However, the large velocity deficit variations observed in the near wake indicates the sensitivities of HK turbine wakes to environmental/operational parameters. A good understanding of how these parameters drive wake formation and flow recovery is needed for accurate wake predictions.

2 Computational and numerical modelling of HAHT

The key to determining the spacing between HK turbines in arrays is to address challenges faced in numerically modelling the flow physics resulting from complex geometries, moving boundaries, and the complex flow conditions as those illustrated in Figure 3.

2.1 Numerical and analytical modelling of HAHT

Analytical and numerical models offer an alternative to physical scale models for simulating the complex flow physics, including wake dynamics. A number of studies have investigated effective modelling approaches for wind turbine wakes [47–49] and employing a similar approach for hydrokinetic flow fields seems reasonable. For analytical models, e.g., [32,50,51], the self-similar nature of the far wake is exploited to obtain expressions for velocity deficit and turbulence intensity. However, the calculated dissipation rate from these one-dimensional models is a function of wake speed only, resulting in uniform downstream wake profiles [52] independent of the effects of the retaining structure, confined flow and relative turbulence.

Due to recent developments in tidal energy, multiple large-scale analyses of tidal turbine arrays have been reported. The majority of the studies utilise simplified numerical models for array scheme analysis [19,53–55]. BEM theory is often used for simplified performance analysis. However, this method does not include any wake effect from the freestream or bounded flow [56]. Vortex-lattice and vortex-particle methods [57,58] may be used

to describe the wake vorticity in concentrated sheets of particles. Computational Fluid Dynamics (CFD) simulations make use of generalized actuator disk (AD) or direct geometry modelling techniques to model complex external effects and more accurately retain fluid structure and wall effects [23]. Additionally, BEM may be embedded in the CFD domain.

CFD models may be used to resolve the effect of turbulence at sub-grid scale level. Due to this, they are being used more often for first order analysis or design, many without experimental validation. However, they have the potential to offer more comprehensive solutions and insight when their limitations are understood.

2.2 CFD modelling for HAHT

For CFD wake analysis turbulence models are selected to model the turbulent structures in the wake which ultimately drive wake dissipation. The near wake may be characterized as a connected structure associated with vortex shedding similar to the Karman vortex street behaviour [59]. In the far wake two primary features exist in the wake, low water speed and high turbulence intensity [60] the former of which reduces the power output of any subsequent turbine placed in its wake. Accurately representing turbulent flow in CFD remains a large challenge due to its strong dependence on initial conditions as well as the wide range of scales (eddies) present in the flow. Most often statistical approaches based on the RANS equations, with eddy viscosity models for turbulence closure, are used [61,62]

Previously, Shives & Crawford [63] indicated the k-ε model predicts much faster wake recovery than experimental results. Employing the shear stress transport (SST) k-ω model improved on this. However, it overcompensates, resulting in a delayed wake recovery. In summary the spatial pattern of turbulence in the wake was improved but the intensity was still too low. A possible solution may be to specify minimum turbulence intensities or limit decay [63]. Freestream turbulence defining input factors may vary over different CFD codes. Many assign default values and allow the user the override these if desired, however usually little guidance is available on the effect of these choices on decay rates [48]. This is especially true for the SST, k-ω and k-ε models where the specified turbulent dissipation rate strongly affects the development of the wake and dissipation curve.

In many scenarios eddy viscosity models are an attractive, well-calibrated option (specifically performance focussed studies). However, cases where flows with strong swirl or streamline curvature exist, or where secondary motion is driven by turbulence anisotropies, these models cannot provide the information required to accurately compute physical effects [64]. In the past this problem has been alleviated by moving beyond the eddy viscosity models to Reynolds Stress model's (RSM). However, these models have shown reduced numerical robustness especially when equations are integrated through the viscous sublayer [64]. McNaughton [65] performed a comparative analysis (near wake and turbine performance) using two 2-equation eddy viscosity models and the Launder-Reece-Rodi (LRR) Reynold stress model and concluded further testing needs to be completed on requirements of grid refinement in the wake when utilizing RSM's. The study found the SST and LRR methods performed well when compared to Large Eddy Simulation (LES) results.

A higher-level solution is possible with LES which is a scale-resolving simulation. This means a portion of the turbulence spectrum is resolved, not modelled, as in RANS [23]. However, this is yet to replace RANS due to the high-resolution and consequent high-computational demands for wall-bounded flows. Even though LES has remained a research tool to applications not much affected by wall boundary layers (e.g. Combustion chambers) [23,66], it may be useful when analysing details in the flow features [29,66].

Detached Eddy Simulation (DES) proposed by Spalart et al. [67] utilizes a hybrid RANS-LES. This approach allows a decreased grid resolution, eliminating the main limitations of LES. This means the wall boundary layers are covered by a RANS model and free-shear flows computed in LES. DES may result in a reduction of the eddy viscosity without proper generation of turbulent content (which occurs for wall boundary layers) [64]. Salunkhe et al. [14] compared unsteady-RANS (URANS) to improved Delayed-DES (IDDES) for a full rotor geometry model and found that although all models overpredicted the wake diffusion after 4 D downstream, URANS

performed better than IDDES. DES also suffers from a modelled stress depletion issue in the wake, resulting in inaccuracies.

Actuator disk (AD) embedded CFD methods may be useful where large scale flow effects (such as those in multi-turbine arrays) are of interest [35]. Blackmore et al. [68] used a LES approach coupled with an AD to model the wake of a horizontal axis turbine, the results correlated well with published experimental data beyond 3 D downstream. Kang et al. [69] analysed a detailed comparison of AD embedded LES showing that this is not sufficient to correctly reproduce the development of an actual turbine wake. They have proven even in fully turbulent open channel flow; the development of the far wake is sensitive to the stability of the vortical structures in the near wake region. As a result models need to be resolved in detail in the near wake region to predict an accurate far wake result [19]. The AD concept is not applicable for detailed design of a turbine rotor. It may however be useful for wake analysis and allows a significant reduction in computational size and cost [70,71].

Wake formation may not be extremely sensitive to small changes in turbine operation. However, power production has been proven to directly affect the wake velocity deficit, where higher power production produces a higher deficit in the wake [14]. Therefore, the turbine representation should be correctly captured when employing CFD models for wake analysis by incorporating the rotation of the blades and its effect on the surrounding flow field. As the blades rotate the surrounding fluid exerts a force (torque) on the blades, as a result the fluid behind the rotor loses kinetic energy (the wake) and a pressure differential is generated across the blades. The torque enforced is counteracted by the generator keeping a constant angular velocity [72]. Options ranging in complexity and varying in input requirements may be selected. The most accurate rotor modelling technique is modelling the full turbine rotor geometry (FRG). Previous studies indicated this method predicts turbine performance well for lower water speeds and tip speed ratios; however, underprediction of power output may occur at higher velocities. This can be explained by incorrect capture of the strongly separated flow by insufficient mesh resolutions and limitations of the employed turbulence model [23].

Another rotor modelling approach is to distribute a theoretical approach or source term over a virtual disk (VD), replicating the effects of the turbine action and coupling this with a CFD environment. The AD treatment is the least computationally expensive method and applies a uniform force to the flow. However due to the low fidelity modelling option important representations such a rotor swirl are lost [73]. BEM theory on the VD as a mid-fidelity modelling method, incorporating rotational components, and using real turbine geometric data. A limitation of this method is the inability to represent the discrete blade effects such as tip vortices [46]. The BEM-CFD method requires pre-determined lift and drag coefficients (F_L and F_D as inputs as shown in Figure 4).

An important aspect when utilizing the BEM method is incorporating the tip loss correction factor [74–76]. Tip-loss correction compensates when the flow induction factor is large at a specific blade position, meaning the lift force will be almost normal to the rotor plane. Thus, the tangential component of lift will be small, and so will its contribution to torque. The result is a reduced torque and reduced power output (known as tip loss as it only occurs on the outermost part of the blades) [77]. Details of the BEM-CFD method are covered in [46].

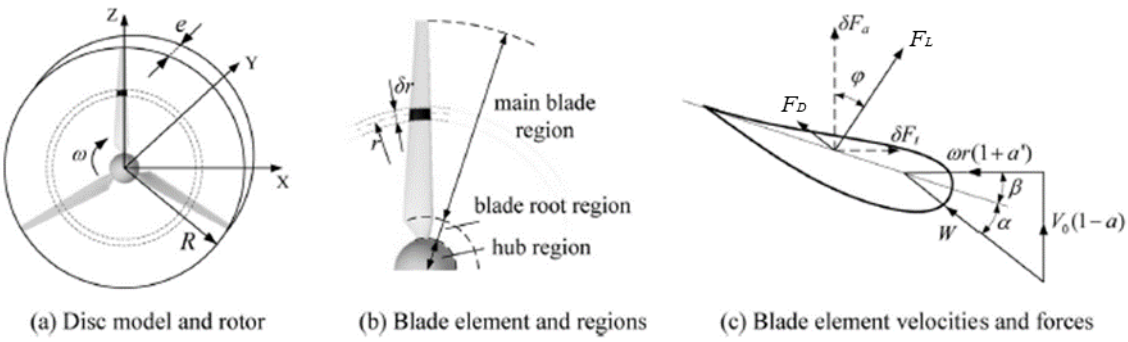

Figure 4: Schematic of the virtual disc model, hydrofoil and blade element characteristics. [78]

A number of recent studies use the BEM-CFD method [76,78–80]. It has been widely used in wind turbine array models with good representation of the wake [46,81]. Various authors [73,82] have used this method to analyse the flow field of turbines arranged in arrays, specifically for tidal optimisation. The SST k-ω model coupled with BEM has been found capable of predicting the flow velocity structures in the far wake regions to an acceptable level of accuracy [46,82]. Gotelli et al. [55] and Gajardo et al. [83] found better agreement of a coupled BEM-DES method than the BEM-RANS method on a 3-bladed horizontal axis turbine. However, Gotelli et al. [55] predicted large variances in the near wake due to the BEM approach but showed better agreement from a distance 3 D downstream.

2.3 Ambient inflow and environmental conditions

The effects of a HK turbine on ambient inflow conditions has been studied in recent years as reviewed in [4]. These studies include the velocity deficit [32,81]; the complex three-dimensional flow structure (including hub and tip vortices) [84]; increase in turbulence intensity and anisotropy[26,40,85]; effects of ambient turbulence levels; unsteady loading; flow depth to turbine diameter; and turbine operating conditions affecting thrust (e.g., tip-speed-ratio) [86,87].

Turbulent, ambient inflow characteristics of depth-limited flows and their implications for HK turbine deployments, are detailed in [2]. Measured vertical profiles of the mean velocity and turbulence stresses reported in literature for rivers and large canals are compared along with classical models developed for turbulent flat plate boundary layer flows. The vertical mean velocity profiles are modelled reasonably well with a power law (exponent = 1/6), and similarly vertical profiles of turbulence (Reynolds) stresses with semi-empirical exponential decay formulae derived from classical open channel hydraulics experiments [88]. Nevertheless, a significant amount of scatter is observed about these modelled profiles due to variations in bedforms, complex bathymetry, non-stationary (unsteady) phenomena, and potentially, three-dimensional flow structures, e.g., large coherent motions emanating from natural and manmade obstructions [89].

Additional to inlet conditions, the consideration of environmental variables on wake prediction and modelling, such as bounded flow and depth below the free surface, is also necessary. Previous studies have specifically addressed the concern of distance to the free surface, as well as blockage ratio [17,18,90,91]. Complexities arise when turbines are placed near the free-surface, as the boundary may modify the turbine flow-field and affect device performance. Generally, this causes significant flow acceleration, its magnitude depending on the blockage ratio.

El Fajri, et al., [92] investigated the effects of shallow water on the near wake recovery through a validated CFD model with a tip clearance of 0.35D. The stanchion holding the turbine in place (Figure 5) initiated the free-surface wake interaction and a significant wake deformation can be seen at 7 D. The results found suggest the free-surface blockage enhances wake recovery in the near or intermediate wake by accelerating the flow in the upper bypass region. However, the wake recovery rate (specifically in the intermediate-far wake) was not affected significantly

as shown in (c) in Figure 5. Kolekar and Banerjee [17] studied this effect and found that smaller tip clearances retarded wake propagation, but accelerated the flow in the upper bypass region. This caused a skewed wake. Experimental investigations proved that small clearances may also cause free surface deformation resulting in a free-surface drop behind the turbine. However, clearances avoiding this behaviour are usually be prescribed by turbine manufacturers to prevent performance degradation. Additionally, an optimal clearance depth (depth form blade tip to free surface) exists, resulting in improved turbine performance [17].

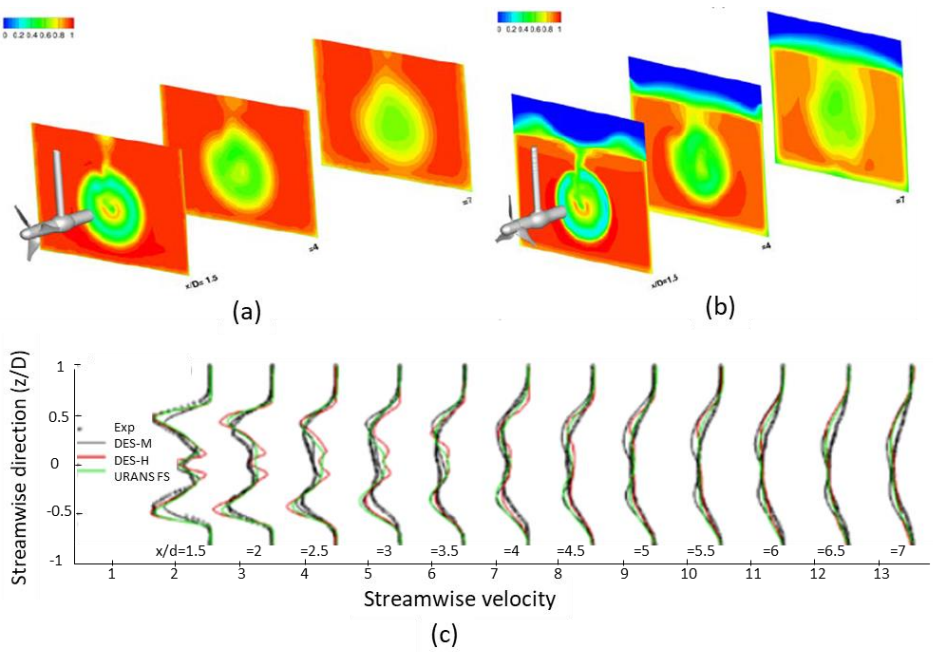

Figure 5: Free surface effect on wake indicated by the differences in (a) single phase-*DES-M/H* and (b) multiphase- *URANS FS* [92]

When a turbine is placed in bounded flow, the flow velocity in the bypass region around the turbine will be increased due to the spatial restrictions of the channel bed and walls as well as the free surface. This change may lead to an altered wake velocity deficit comparing to unbounded flow cases. This effect is caused by changes in the rate of mixing between the wake and the bypass flow (which is the driving force for flow recovery) and thus affects the wake recovery length scale [93]. To ensure accurate prediction of this behaviour it should be ensured that wall effects and boundary layers are accurately modelled.

Ensuring Reynolds uniformity is important within wake studies. Models validated further from the Reynolds number experienced at full-scale results in a lack of confidence in the models [94]. A previous analysis to observe Reynolds dependence using towing tank tests [94] indicated that near-wake statistics (mean velocity, turbulence intensity, Reynolds stress) were less Reynolds dependant than the performance measure of the turbine. However, it is important to consider Reynolds dependencies when scaled models are used for numerical validation. The study also found that when scaling experimental tests, no significant Reynolds number dependence was found for velocity profiles, however a small Reynolds dependence existed for turbulence intensity and Reynolds stresses. Numerical results (specifically using the SST k-ω solution) indicated a stronger Reynolds dependence, overpredicting performance due to the increased blockage and exclusion of tip effects. Previous results have also indicated that power coefficients (C_P) are more sensitive to Reynolds dependency than the thrust coefficient (C_T), the same is true for blockage ratios [95]. In conclusion low blockage may alter the Reynolds number (comparing to non-blocked cases) for scaled tests, and in turn alter the turbine performance. Reynolds uniform
+mity should therefore be included if scaled testing is used.

3 Methods

3.1 RM1 validation case

To allow accurate development of a CFD model, verification (correct numerical model) and validation is necessary. The latter requires comparison with experimental data or numerical data. The Reference model 1 (RM1) turbine [96] with properties as seen in Figure **6** was used as a validation case. The RM1 design and testing environment allows a Reynolds uniform analysis of the inter-effect between the two closely spaced turbine rotor wakes as well as incorporating the effect of turbine wake interaction with the center stanchion itself. The rotor diameter and blade profile resemble those often used in inland hydrokinetic applications. Channel conditions as well as the blockage ratio also hold value for the analysis of inland schemes.

Parameter	**Scaled model**
Flow rate	2.425 m^3/s
Depth	1.0 m
Velocity (hub)	1.04 m/s
Froude number	0.28
Re_c at $C_{p\text{-}Opt}$	$3.1x10^5$
Re_D	$4.4x10^5$
NACA	4415
Diameter	0.5 m
Depth to hub (h_{hub})	0.5 m
Tip speed ratio	1-9

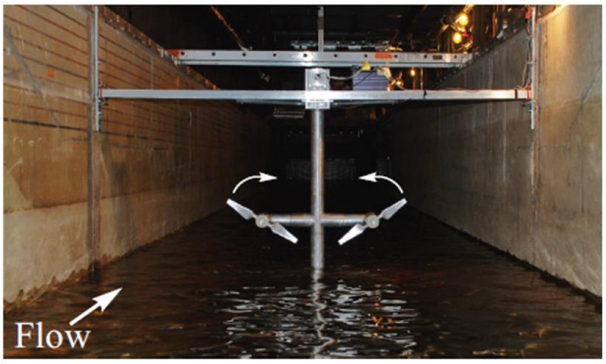

Figure 6**: RM1 laboratory setup details** [16]

Mean and fluctuating velocity fields were measured using three Nortek vectrino ADV's sampled at 200 Hz data output at hub height. To ensure any ADV measurement volume rotation was considered, the channel was ponded with water and a towing test performed to determine the rotation. The rotation matrix was then applied to all measured data before calculation of flow statistics. Additionally, time series data was filtered to remove erroneous samples [97]. The measured turbulence intensity in the rotor region was approximately 5%. Wake vertical velocity profiles were taken downstream of the turbine from 1 D to 10 D at intervals of 1 D. These were collected for 3 min at 200 Hz. A horizontal plane was collected from 1 D to 10 D also with 1 D spacing, the cross stream ADV point locations were assumed to have provided enough spatial resolution to capture key characteristics of the wake. The velocity time series was decomposed into mean and fluctuating components through Reynolds decomposition, the fluctuating velocity components were used to calculate flow statistics such as turbulence intensity, Reynolds stresses and turbulent kinetic energy. Details may be seen in experimental reports [16,96].

Both rotors (counter-rotating) were identical but performed differently (Figure 4). The flow complexity in the channel, as well as the slight asymmetry in the approach flow could have affected this change. Because of the performance sensitivity to velocity (U^3) a slight difference in approach velocity (3-5% e.g., 0.03 m/s) could cause a 10% change in performance (at optimal TSR). A variation of wake results in the near wake was also observed, with a 17% higher peak velocity deficit for the left rotor at 2 D downstream. This emphasizes the strong variability in near wake results from small operational changes, asymmetric inflow conditions or manufacturing flaws.

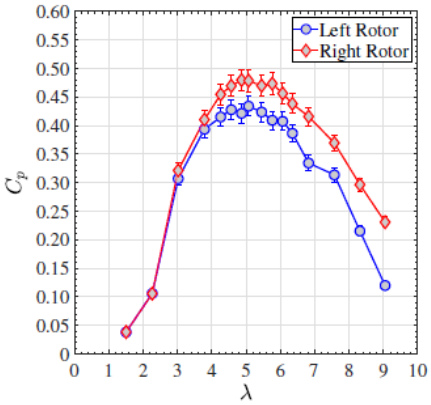

Figure 7: Calculated power coefficient (C_p) versus tip speed ratio (λ) for left and right rotors, dashed lines represent results before calibration [16]

3.2 Numerical domain

Commercial modelling software Siemens STAR-CCM+ was used to simulate the wake effects of the turbine. This allows comparison of commercial software used in HAHT design. The computational domain can be seen in Figure 8. The RM1 dimensions were replicated using a wall bounded model. The domain extended from -8 D upstream to 30 D downstream of the axis of rotation. The inlet length was selected to allow full flow development (including wall boundary layer development) before the rotor is reached. Similarly, the outlet length ensured the channel outlet boundary has no influence on the wake dynamics, although this large distance is not necessary for performance analysis (around 15 D is adequate [98,99]). The large downstream length was selected to allow analysis of far wake accuracy. A velocity inlet and downstream pressure outlet were specified as boundary conditions. The turbulence and velocity values measured in the experimental analysis were specified at the inlet. Full development of the boundary layer on all surfaces (boundary walls, blades, and stanchion) was ensured through the specific turbulence model wall treatment and mesh resolution for each test case.

The rotor was modelled using two widely used methods. First the overset (sliding) mesh technique was used to deal with the blade movement, this method was employed in numerous validated axial turbine studies [37]. The presence of the blades is taken into account by discretising the blade geometry on a computational mesh [37,83]. During each time step interpolation of the flow field is performed between the first cell mesh of the moving body and the background mesh region (Figure 10C). The sliding mesh boundary can be seen on Figure 10B. The rotating mesh continua should be a minimal size to ensure numerical efficiency whilst also ensuring numerical stability. A cylindrical area 10% larger than the turbine diameter was used here. Second, a VD was used (Figure 11B) and a BEM model was employed. This VD-BEM modelling approach has demonstrated good accuracy at reduced computational cost [76,78–80]. A BEM tip-loss correction was incorporated using the Prandtl tip loss correction method [75].

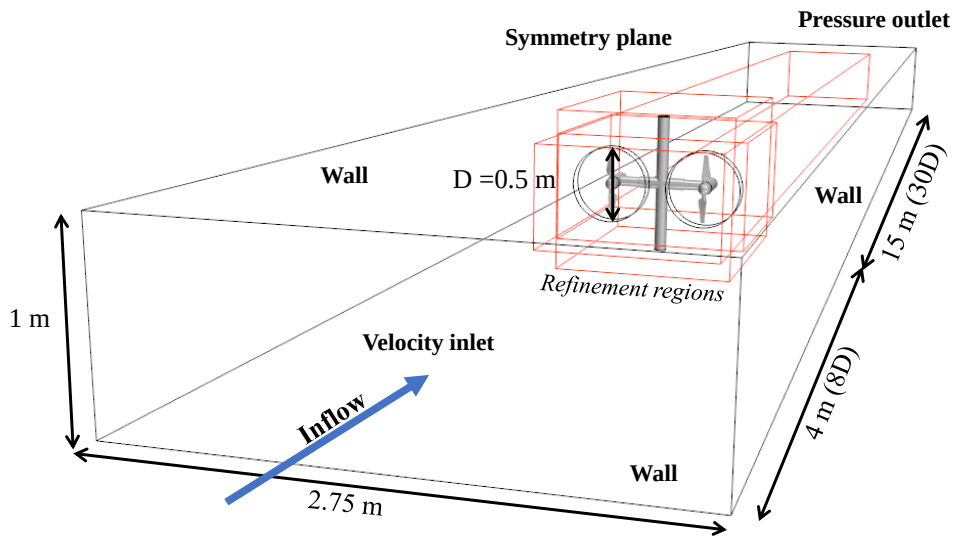

Figure 8: Computational domain

Careful selection of flow physics, and comparisons of commonly used models is a crucial factor in accurate modelling of these complex flow fields. RANS eddy viscosity models are most often used for turbine analysis [63,100–102]. The k-ε turbulence model was compared to Menter's SST k-ω turbulence model [103] which typically predicts adverse pressure gradients in the near wall region better than the k-ε turbulence model. The near wall region is defined as the viscous sublayer in the region $y^+<5$, where $y^+= yu^*/\nu$, y is the normal distance from the wall in wall coordinates, u* is the friction velocity and ν is the fluid kinematic viscosity [104] [103]. Both models were built with a different mesh, specifically in the wall regions, the k- ε model was built using a high y^+ approach and resolving boundary layers, whilst for the SST k-ω turbulence model a low y^+ approach was used, fully resolving the viscous sub-layer. More complex Reynolds stress models (RSM) were then employed to allow more accuracy in prediction of possible flow anisotropy, these have shown positive results in HK wakes but require further validation [65]. The RS Linear pressure strain two-layer (RS-LPS2) model [105,106] was selected which allowed near wake accuracy with a low y^+ wall treatment on the turbine and turbine structure.

Steady and transient simulations were performed (for both RANS and RSM) where unsteady terms were discretized using a 2nd order implicit scheme. A time step ensuring Courant numbers less than 1 in all regions was ensured as far as possible. The time steps were around 0.002% of the total time to complete one rotation for the FRG simulations and 0.01% for the BEM-CFD models. However, timesteps varied over each approach depending on the results of the grid convergence index (GCI). All approaches are shown in Figure 9, where combinations of model properties were varied with the goal of understanding the limitations as well as capabilities of each approach.

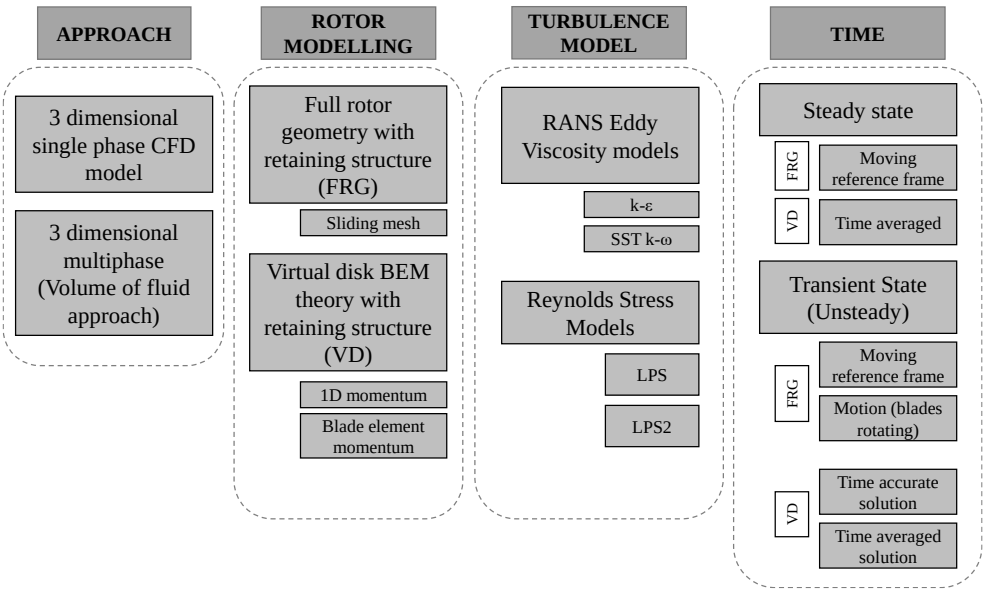

Figure 9: Summary of CFD approaches

3.3 Mesh

The computational domain (Figure 8) consisted of a polyhedral mesh with grid refinements in the near wake, far wake and surrounding the retaining structure. Past results indicate the importance of fine grids to track the tip vortices when using simplified RANS models [23]. Simulations were performed on various meshes with similar base sizes and increased resolution over volumetric controls in regions of high turbulence. An adaption of the GCI [107] was used due to the variance in grid sensitivity in the different wake regions, therefore separate regions were decreased incrementally, starting from the near wake region, until no changes in wake behaviour was observed. For the optimum flow conditions (λ=5.07) results showed grid sensitivity up to a minimum cell size of 3 mm (0.6% D) around the blades for FRG. However, a further 30% increase in cell size showed only a 1% change in wake dissipation rate. For FRG a small mesh size is inevitable to capture the geometry of the blades (under high rotation) as well as boundary layer formation. RS models also required finer grids comparing to eddy viscosity models. For the RM1 turbine the advancing prism layer Mesher proved to be best for the complex geometry and customization of the prism layer thickness on the upstream and downstream side of the blades. The mesh can be seen in Figure 10. Final mesh sizes were around 19 million cells.

For the VD model (Figure 11) a 10 mm minimum cell size (2% D) proved adequate for a BEM-RANS analysis. The finite number of blades across the virtual disk should ensure introduction of the effects of the propeller on the computational domain. A minimum of 4 cells over the blade thickness were ensured with all meshes, further refinement or change in thickness did not affect results. Both rotor modelling techniques showed converged solutions for near wake cell sizes of 8 mm. Increasing this near wake grid by only 4% (2 mm cell size change) resulted in a 5% change in wake velocity deficit results. Therefore, near wake grid sensitivity should be carefully considered. A far wake cell size of around 8-15 mm showed no significant change. In this paper, a 14 mm (2.8% D) base size in the far wake was selected. Final mesh sizes were around 13 million cells.

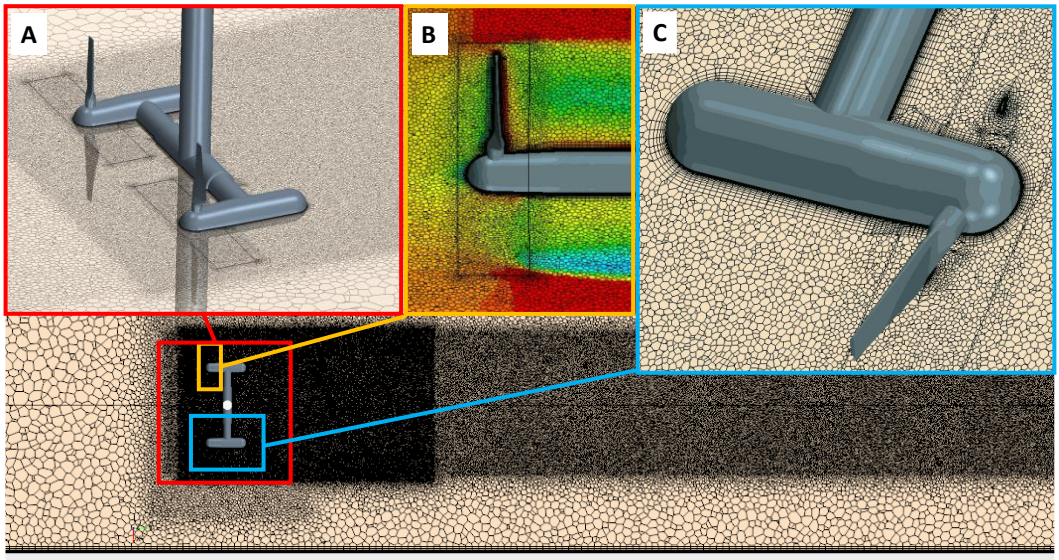

Figure 10: Full rotor geometry mesh A) full rotor B) Sliding mesh interface C) Dynamic mesh

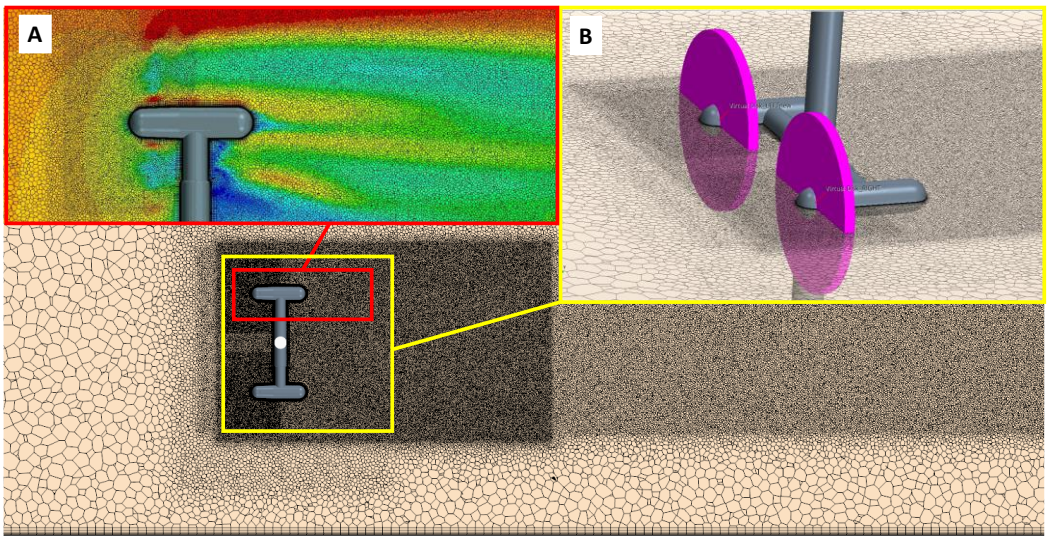

Figure 11: BEM-RANS Mesh A) velocity contour on BEM mesh B) Virtual disks.

3.4 Boundary conditions

Walls were modelled with non-slip conditions which allowed formation of a boundary layer, and incorporation of bounded flow effects. Prism layers were built according to the wall treatment requirements applicable to each model. For the SST k-ω models high y^+ treatment ($30<y^+<300$) on the channel walls, and a layer resolving low y^+ ($y^+<1$) approach on the turbine and retaining structure was built. Mesh refinement, specifically in the near wall region of the boundary layer is crucial for accurate near wake region development, especially where both separated and attached flow exists [34]. Gibson & Launder [108] investigated the pressure fluctuation effects of capturing the boundary layer and noted the importance of an accurate capture of boundary layer formation and thus developed a two layer formulation which may be applied to the linear pressure strain model (LPS2 model). All analyses used the two-layer formulation.

Simulating the water-air interface (free surface) has been approached in various ways in literature. Most often the free surface is assumed to be a significant distance from the turbine and so free surface deformation is neglected and a symmetry boundary condition is used. Computational cost is saved using this approach [76] compared to a more accurate boundary condition where the free surface is modelled. Both were analysed in this study.

4 Results and discussion

4.1 Performance comparison

For HK turbine performance analysis both steady and transient FRG and BEM rotor modelling approaches are often employed and have proven good correlation to experimental results with the approaches used in Section 3 [76,79,109]. Numerous studies have assessed which models are best for performance tests [62,71,101,110]. Although the focus of this paper is on modelling of the wake dissipation rate, accuracy of each model's energy capture was ensured through comparison to experimental performance variables. Table 1 includes the torque (T) and power co-efficient's (C_P) measurements and model results for the optimum TSR. The CFD results for both rotors showed identical results and thus only one set of results is listed. Due to the uncertainties of accuracy of the experimental performance results, specifically on the left rotor (mentioned in 3.1) a certain degree of uncertainty lies on the measured values. However, the CFD results all lie well within the measured range and within 5% of the measured results. A similar conclusion was found by Masters et al. [73]. The experimental systematic and random measurement errors existing on the torque sensors were also included, these were calculated based on measured and expected value comparisons.

Table 1: Performance comparison

ROTOR	**Experimental**			
	T (N.m)	T Error (%) (sensor calibration)	C_P (%)	
left	2.081	3.80%	41.20%	
right	2.603	0.69%	47.60%	
Turbulence model	**FRG-CFD**			
	Steady (moving reference frame)		Transient (motion)	
	T (N.m)	C_P (%)	T (N.m)	C_P (%)
RS-LPS2	2.35	44%	2.39	45%
SST kw	2.35	44%	2.45	46%
k-ε	2.16	41%	2.28	43%
Turbulence model	**BEM-CFD**			
	Steady state (time averaged)		Transient (Time accurate)	
	T (N.m)	C_P (%)	T (N.m)	C_P (%)
RS-LPS2	2.43	46%	2.38	45%
SST kw	2.43	46%	2.38	45%

4.2 Rotor modelling

By modelling the FRG using the sliding mesh technique, the vorticity in the wake is simulated (Figure 13). The tight vortical structures observed in Figure 12 correlates with the expected near wake behaviour prevalent in past LES studies [22]. For steady state analysis a moving reference frame (MRF) is used to enforce the turbine rotation, however the solution lacks adequate simulation of the vorticity and rotation in the wake. From Figure 13 it is clear the transient solutions better capture the wake. Although it may seem that steady state results better align with the left rotor it should be noted that during laboratory testing the left rotor did not perform to the expected degree of accuracy and has a larger degree of error [111] (hypothesized to be a result of approach flow asymmetry [16]). The steady solution indicates a high initial turbulence with an overpredicted velocity deficit in the near wake. This resulted in an accelerated and inaccurate wake dissipation rate. Accelerated decay of the turbulent kinetic energy (TKE) of the bypass flow was prevalent in the near wake region. This may be attributed to the simplification of eddy viscosity model and its inability to resolving small eddies forming at the tip and root vortices. The eddy-viscosity model showed a strong vortex structure extending from the blade tips which is maintained up to 6 D

downstream due to inadequate mixing in the model [65]. This leads to inadequate wake dissipation as the TKE in the bypass flow is too weak to break these structures down in the near wake.

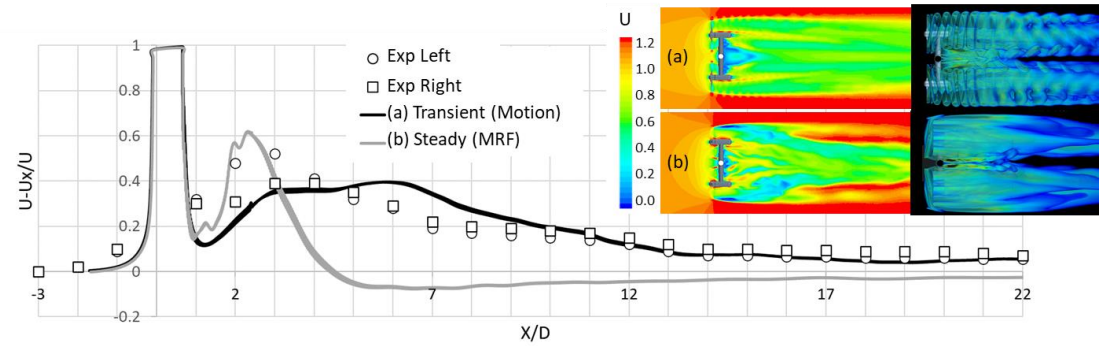

Figure 12: Comparison of steady state vs transient results for the FRG-RSM dissipation rate as well as velocity magnitude and vorticity scalar scenes (CFD results are identical for left and right rotor).

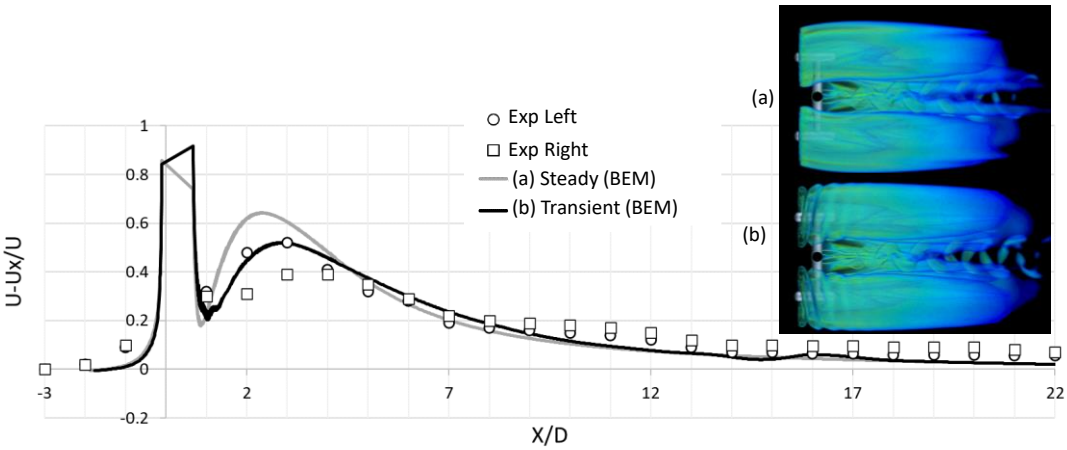

Figure 13: Comparison of steady state vs transient results for BEM-RSM dissipation rate and vorticity scalar scenes (CFD results are identical for left and right rotor).

Although simplified rotor modelling using a VD reduces computational time, the simplification results in the lack of tip and root vortices formation (seen on the vorticity plots in Figure 13). This is a result of the BEM-VD theory, where a force (which is a function of the rotor hydrofoil geometry) is applied at all locations along the disk and blade tips are not resolved. The BEM-VD time accurate approach available in most commercial software improves this prediction. This method tracks the motion of the blades adding a source term only to the volume of cells corresponding to the location of the blades (specified as input values to the VD). The improvement when using a time-accurate transient approach can be seen in Figure 13. Similar behaviour as that shown in FRG modelling occurs, however the effect is not as pronounced.

For BEM-VD rotor modelling a sensitivity analysis was done using drag (C_D) and life (C_L) coefficients comparing experimental [112,113] and numerical data (XFOIL data). The results indicated a significant variation in turbine performance, wake formation and wake dissipation rate in the near and far wake. Better results were obtained when using numerical coefficients over a broad range of Reynolds numbers (including the operational range) and angle of attacks. Therefore, it is crucial that extensive and well approximated data be used. All BEM-VD results utilized the Prandtl cosine tip loss function, not considering the tip loss effect of the turbine resulted in a further 12% overestimation of the near wake velocity deficit.

Although modelling the full rotor geometry should intuitively increase the accuracy when comparing to a VD approach, it is hypothesized that the complexities in fully modelling the geometry with these lower fidelity closure models results in a less accurate wake solution. Meaning the VD approach couples better with RS models as the

modelled wake vorticity from the VD is easily broken down by the TKE present in the wake and does not depend on resolving the smaller eddies which are present and important in real wake conditions. Higher fidelity models such as LES's have shown FRG modelling gives a better approximation of the wake behaviour. It is also important to note that although steady state models may be sufficient for performance analysis, wake analysis requires a transient approach.

4.3 Dissipation rate

Hub height velocity measurements are often used as an indicator of wake recovery. A CFD approach accurately capturing the recovery rate and behaviour would be most useful for device scale analysis of HAHT systems. A summary of the hub height velocity deficits for the various transient modelling approaches investigated in this study can be seen in Figure 14. No velocity deficit difference was observed in wake results between left and right rotors in the CFD models, thus only one set of numerical results are plotted together with both left and right rotor results from the experimental analysis. The discretion between rotos in the experimental wake velocity deficit becomes almost insignificant after 4 D after which little variation is observed.

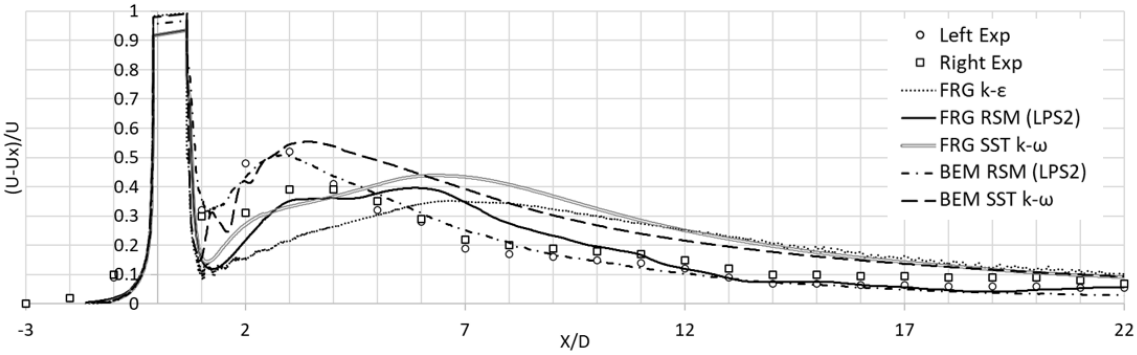

Figure 14: Comparison of RANS modelling approaches for left and right rotors.

The wake behaviour observed is characterized by a tight vortex formation in the near wake which starts to mix with the bypass flow further downstream. This mixing behaviour results in dissipation of the wake as it is carried downstream. Mixing is then slowed after about 10 D downstream where approximately 80% wake recovery has occurred. The remaining deficit is carried a significant distance downstream.

For the FRG modelling all RANS solutions proved to have the similar problem of accelerated decay of the TKE in the bypass flow. Comparison of the wake width, vortex formation as well as dissipation rate indicated these models (k-ε and SST k-ω) predicted the largest dissimilarity to experimental results in terms of dissipation rate. Although turbine performance was adequately determined, adequate capture of the wake dissipation rate was limited. The SST k-ω showed better prediction than the k-ε model. However, it still overpredicted the wake by up to 20% between 6 D and 10 D downstream and significantly delayed wake recovery.

Employing the RS-LPS2 turbulence model significantly improved predictions with an improved mixing rate in the near wake and good correlation to experimental results after 10 D (Figure 15). The improvement could be attributed to the RSM's transport equations accounting for the effects of turbulence anisotropy [105,106]. Whereas eddy viscosity models use the Boussinesq hypothesis [64] which assumes isotropic conditions. For LPS2 results accelerated TKE decay in the bypass flow is still observed with inaccurate prediction of dissipating wake behaviour up to 10 D. Although the RS models are known to have more accuracy within turbulence description, they also have limitations in predicting turbulence for complicated flows, especially in describing the effects of rotation [114]. Curvature correction factors are available in some commercial codes and may be a useful tool in some cases. For this investigation, the correction did not have a significant effect. For all RANS solutions inaccurate wake results may also be attributed to the lack of resolving small eddies, which can only be fixed by employing higher fidelity models such as DES or LES.

When coupling BEM-AD with SST k-ω or LPS2 similar behaviour is observed. For the SST k-ω solution, a high velocity deficit is observed in the near wake, resulting in a delayed wake dissipation, and predicting inaccuracies up to 17 D downstream. An accumulated effect is observed through the shortcomings of the VD, which generally over estimates the turbulent eddy viscosity in the high shear flow within the VD and near wake [63]. This induces rapid mixing in the near wake and a higher peak velocity deficit.

The BEM-LPS2 turbulence model showed best correlation to experimental results behind the turbine rotor with a maximum difference of 4% between 3 D and 17 D downstream (Figure 15). The theoretical modelling of the turbine rotor (using a VD) does not produce strong tip vortices. Although this is a shortcoming of utilizing the BEM-VD approach, when coupled with a RANS solution, the weaker vorticity requires less TKE in the bypass flow to break up the rotating wake structure. As a result, inadequate mixing is less of a problem when combining RANS with this simplified rotor technique (Figure 15). The better correlation of the BEM-CFD model may be attributed to the shortcomings of the RANS approaches in the FRG rotating body-fluid interaction rather than greater accuracy when using the VD. When using the BEM-CFD approach less accuracy in resolution of the fluid-blade interaction is needed as the rotation effect on the flow is modelled using the BEM theory and therefore only requires correct resolution of the wake beyond the turbine. Further validation cases should investigate the consistency of this effect for variations of operating conditions.

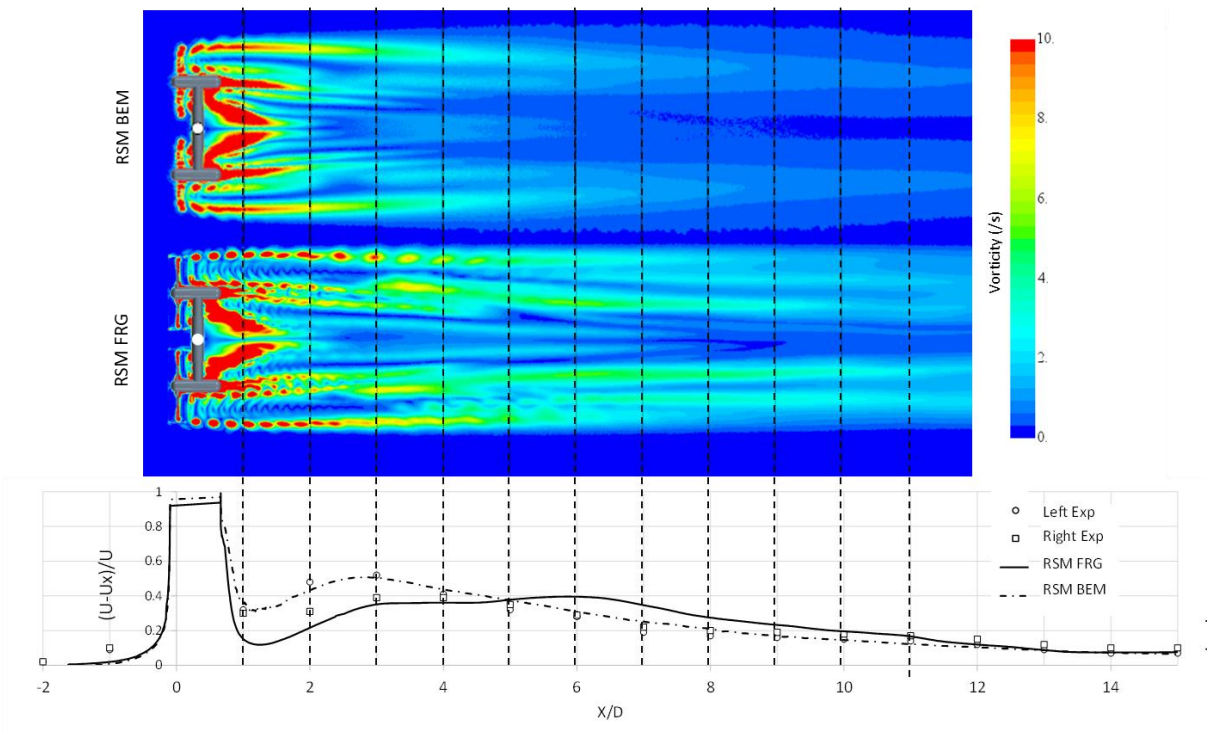

Figure 15: Vortical structure comparison for the rotor modelling techniques (using RS-LPS2 turbulence model)

4.4 Sensitivity to input parameters and boundary conditions.

A major challenge in CFD analysis is the prescription of inlet conditions, especially when validating models with experimental results. Correctly replicating the experimental conditions, including the anisotropy of the turbulence within the inflow boundary is a challenge. It is clear from the equations used to solve turbulence dissipation rate in the SST k-ω model that the chosen freestream values of turbulence quantities have a strong influence on the rate of decay of turbulence [48]. Spalart & Rumsey [48] also demonstrated that eddy viscosity models facilitate more rapid decay of turbulence at higher freestream turbulence intensities (TI), and the same is true for low levels of freestream eddy viscosity. The factor which most affected the recovery rate for all RANS approaches, especially

in the near wake, is the specified inlet turbulence. This effect is portrayed in Figure 16 where the dissipation rate for a high turbulence case (15%) as well as the assumed experimental turbulence case (5%) is compared. Higher turbulence reduced the peak velocity deficit in the near wake, which agrees with previous LES results [85] as well as similar experimental results comparing turbulence cases [24,26].

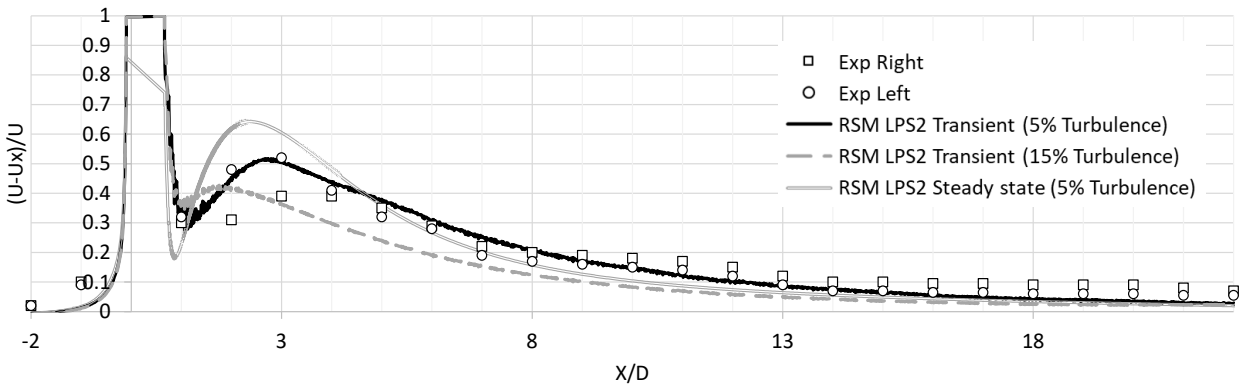

Figure 16: Turbulence input specification effect on wake dissipation rate for BEM-CFD analyses.

The experimental turbulent and velocity profiles (Figure 17) indicate a slight asymmetry about the rotor center. This indicates the free surface as well as channel bed may have an influence on the wake. Although a slight asymmetry is seen in the numerical wake, the effect is more pronounced in experimental conditions [96]. Incorporating an air/water interface may increase the accuracy of capturing the asymmetric effect, but also significantly increases computational overhead [115]. The vertical profile of a multiphase model using the experimentally measured free surface profile at the inlet is shown in Figure 17c. When comparison is drawn to a single-phase model with a symmetry plane boundary condition (in Figure 17b) a slight difference in the velocity profile close to the free surface is observed. Additionally, a slightly accelerated recovery region is seen between 6D-10D downstream in the bypass flow between the wake and free surface. Although this effect was minimal in this case, it may be necessary to perform a multiphase analysis when the turbine is in closer proximity to the free surface. The wake effects of depth variation have been previously investigated for a shallow turbine and can be seen in [42]. Blockage and free surface effects may play a bigger role at higher blockage ratios and cases where turbine performance near the free surface is of importance. When BEM-VD theory is used for scaled tests, blockage correction factors may be incorporated [90].

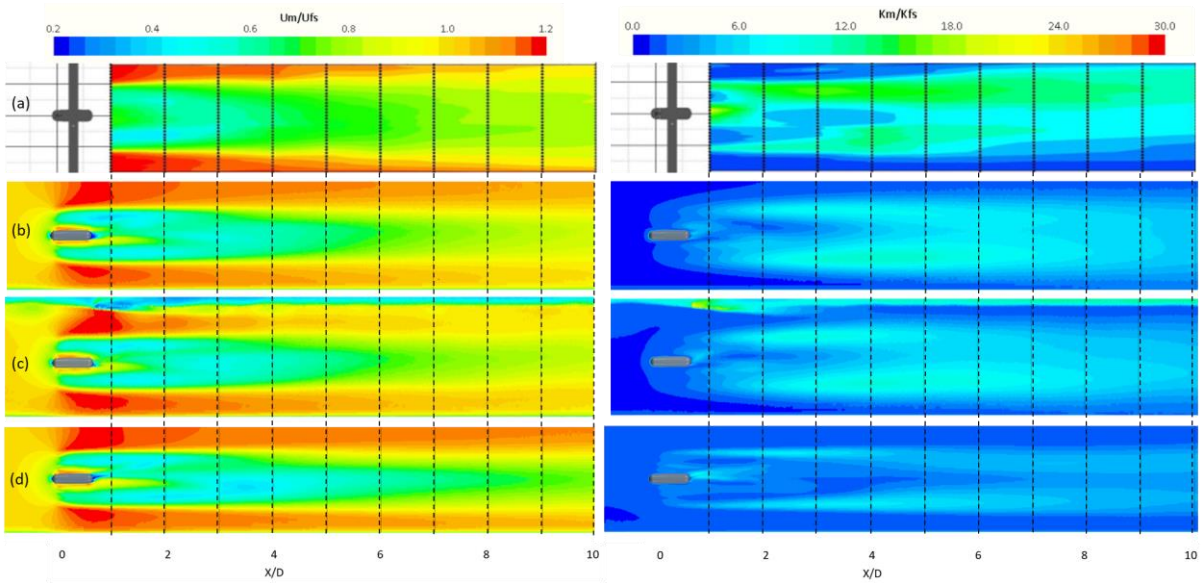

Figure 17: Vertical velocity (left) and turbulence (right) profiles comparing a) Experimental results b) Single phase BEM-RS(LPS2) c) Multiphase BEM-RS(LPS2) and d) Single phase BEM-SST k-ω

The inlet and outlet boundary conditions should correctly model the environmental conditions. Any wall boundaries should be modelled to capture the boundary layer formation upstream of the turbine. If a constant velocity is applied at the inlet, full boundary layer formation (ensuring accurate velocity distribution over the flow area) should be reached before the analysis region. More realistic boundary conditions such as those shown in Neary et al. [2] may be used as inlet conditions to reduce mesh sizes (inlet lengths). Utilizing a constant pressure outlet (used in the single-phase analyses) showed negligible effects when compared to the realistic pressure distributions used in the multiphase downstream boundary. However, a distance of at least 10 D to the outlet was ensured here **(Figure 17).**

Although this paper has shown better results using RS models, due to the reduced computational expense of two-equation eddy viscosity models, it may be beneficial to use these models as a first order estimate and adjust for differences (especially when FRG modelling is necessary). The solution is to prevent accelerated TKE decay. As mentioned previously, eddy viscosity models result in more rapid decay of turbulence at higher freestream TI's, and the same is true for low levels of freestream eddy viscosity. Therefore, to achieve a reasonable turbulence decay rate, very low TI, or very high eddy viscosity value should be chosen for the freestream.

A solution to this may be "controlled decay" where an ambient turbulence source term is enforced over the domain to prevent decay. This may be done by utilising the SST k-ω equation but increasing the turbulent production term or adding a turbulence source term equal to the measured TKE or TI present in the flow field, over the whole domain. This limits turbulence dissipation by subtracting the inflow decay specified and counter-acting turbulent decay. In the validation case, addition of the source term significantly improved results to within 5% accuracy between 4 D and 12 D downstream for the FRG case, where the maximum eddy viscosity model error is observed as shown in Figure 18. Shives & Crawford [63] recommended a more precise solution. To augment the production term in the near wake, specifically for results when a simplified rotor modelling technique is used, and tip vortices are not resolved. However, this is complex and may vary between testing cases. Olczak et al. [44] also improved BEM-CFD results by around 25% through an added turbulence source.

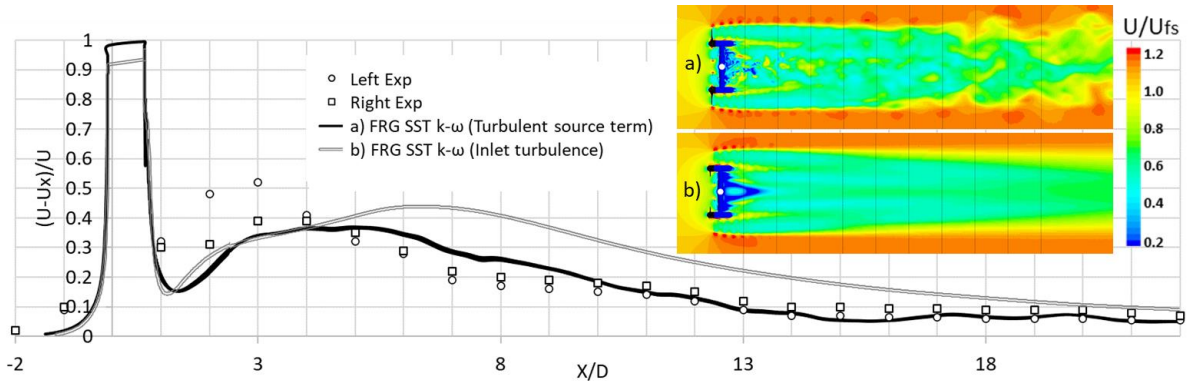

Figure 18: Turbulence source term SST k-ω improvement

4.5 Further validation of prescribed method

For further assurance of the accuracy of the method which is prescribed in this paper an additional bounded flow HAHT experiment was modelled for comparative purposes. The laboratory test results from Mycek et al., [24,26] were used for comparison. The turbine in Figure 19 was modelled using the same approach mentioned in Section 3. Two cases with varying inlet TI's were modelled and the wake dissipation rate results were compared.

Description	Variable
Rotor diameter	0.7 m
Blade profile	NACA 63418
Flow depth	2 m
Tip speed ratios measured	0-10
Flow velocity (V_{hub})	0.8 m/s
Reynolds number	1.4-4.2 x 10^5
Sense of rotation	Counter clockwise

Figure 19: Turbine details and picture [24]

The mesh resolution was consistent with the ratios used in the RM1 validation case. Boundary layers were altered where needed to ensure the correct wall treatment was implemented on each boundary. A timestep of 0.001s was used ensuring a Courant number less than 1 over all cells in the mesh. A transient LPS2-RS turbulence model was used. A result comparison was drawn. The results indicate the hub height centreline velocity deficit downstream of the turbine and contour plots (Figure 20) and the average velocity measured over an area equivalent to the turbine swept area (Yr) at ten points downstream of the turbine (1 D to 10 D as shown in Figure 21). Two sets of experimental results were compared, a low inlet turbulence scenario (with turbulence intensity T= 3%) and a higher inlet turbulence scenario (T=15%).

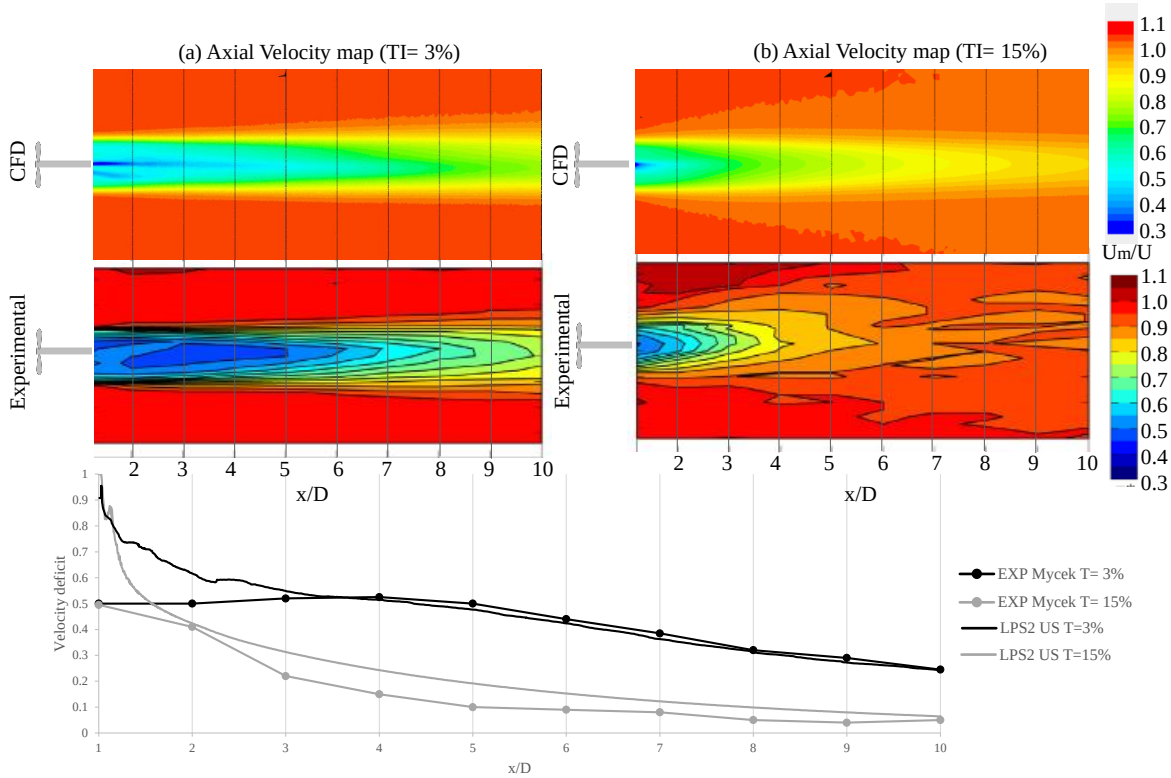

Figure 20: Comparative results of the downstream lines and contour plots for (a) T=3% and (b) T=15%

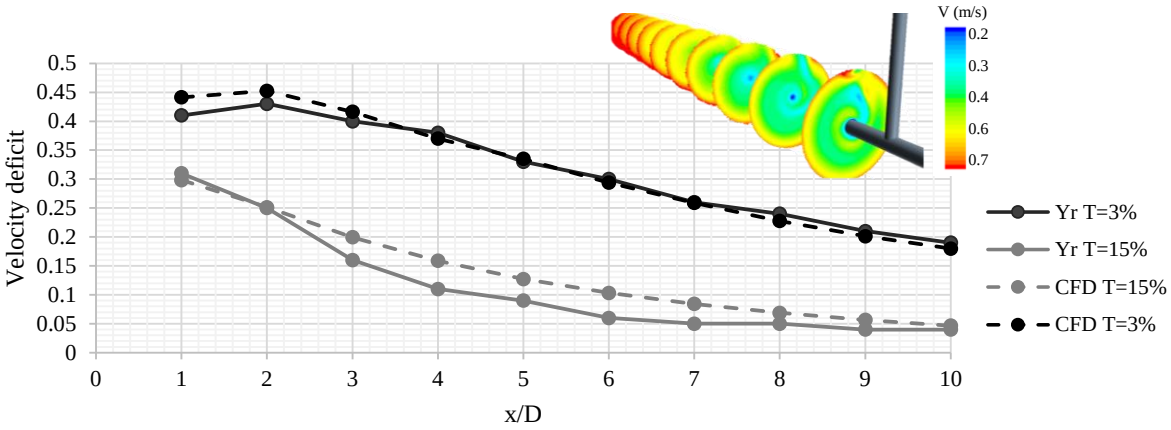

Figure 21: Results for the velocity deficit averaged over the turbine swept area at points downstream

For both the low and high turbulence scenarios a slightly higher velocity deficit was predicted by the CFD model in the near wake (1 D to 3 D). This discrepancy could be attributed to multiple factors, such as mesh size, implemented turbulence model (for the CFD model) as well as experimental measurement error. On close inspection of the wake behind the turbine hub, which extended 1.02 D behind the turbine, a very low velocity zone can is observed directly behind the hub (Figure 22), which is to be expected as flow passes a blunt body. The Karman vortex street behaviour is also seen behind the hub and results in a highly turbulent zone. If this behaviour is predicted correctly, it would make accurate experimental point velocity measurements using probes quite difficult and could thus result in lower velocity measurements. An example of this can be seen in Figure 22 where lines slightly offset from the centreline were used to measure the mean flow velocity downstream over a single rotation. The results varied significantly in the near wake and when used, showed closer correlation to the experimental measurements. This indicates velocity deficit changes up to 50% could occur in the near wake by probe placement inaccuracies of only 50mm (0.07 D). This inaccuracy may be eliminated by using the area averaged velocities (Figure 21) where measurements of velocity deficit were averaged over an area equivalent to the turbine swept area (Yr). This analysis would more likely remove errors made in point velocity measurements and could therefore result in the better correlation observed.

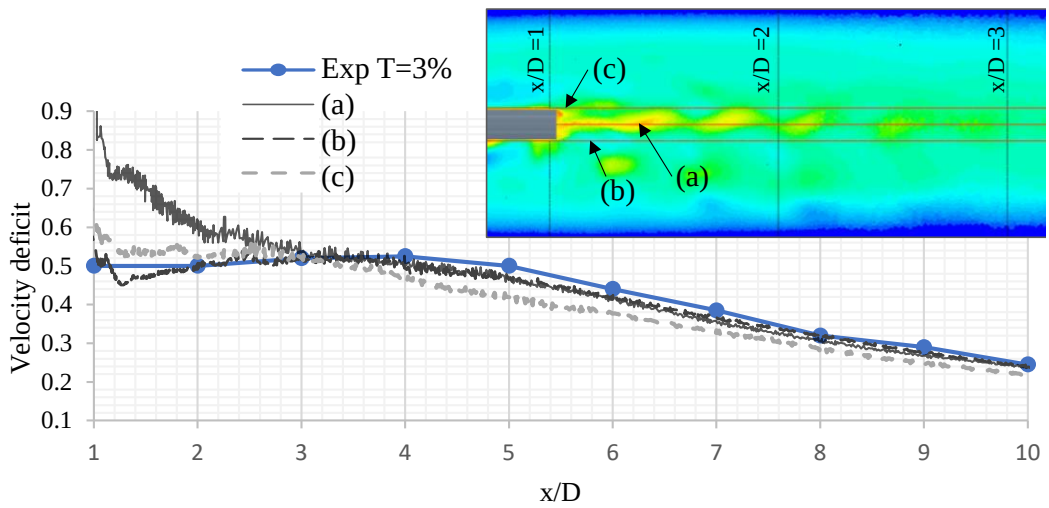

Figure 22: Downstream mean velocity deficit for (a) centreline (b) left offset 0.07 D and (c) right offset 0.07 D and instantaneous velocity contour plot

A slight underestimation of the velocity deficit in the high TI scenario (T=15%) is observed. This could be attributed to the overly rapid dissipation of turbulence resulting from the use of the RS models which also reduced the wake spreading effect observed in the experimental case Figure 20b. This effect may be more pronounced in

higher turbulence cases. Despite this difference the CFD model seems to predict the wake dissipation rate to a relatively high degree of accuracy after 3 D downstream (max error of 4.5% for the T=3% case and 9% for the T=9% case). The model also captures the change in wake behaviour when the inlet turbulence is altered, which is an important input variable in wake analysis.

4.6 Discussion of findings

The review study highlights the importance of a rigorous validation process and using tested computational methods when analysing the effects of HK turbines on wake generation and flow recovery. The following points summarize the key findings:

1] The shortcomings of the employed modelling technique (analytical models, simplified numerical models, CFD models) should be understood and carefully considered. Often too much confidence is placed on results from simplified techniques that have not been properly validated.
2] Simplified techniques may be used where the intention of the model is a specific part/scale where uniformity laws are focused on only relevant areas to decrease required computational resources. Here, the consideration of scales of modelling and ensuring proper validation of the analysis region is important.
3] Correct description of the boundary conditions as well as quantifying the sensitivity of such boundary conditions are crucial for CFD models. In this work the free-surface and blockage effects as well as upstream development of wall boundary layers were of important concern. The complex inlet condition (velocity and turbulent distribution) should be carefully modelled. This is even more important for inland HK device application where spatial constraints give rise to many design limitations.
4] The correct selection and application of turbulence models is important. Research on the applicability of turbulence models within the HK flow environment has increased in recent years, many of which are summarized in this paper. The importance of understanding the applicability and limitations of each model prior to application remains critical, especially as commercial modelling software becomes an increasingly common tool for feasibility studies and design. A carefully researched and prescribed method should be used in such cases (as is a primary purpose of this review).
5] Rotor modelling techniques in CFD applications should be selected together with turbulence models and based on the analysis region. FRG modelling performs well for performance tests but has shown to have shortcomings in wake dissipation accuracy when coupled with RANS models. Simplified disk techniques should only be used when well-defined input parameters (lift and drag coefficients etc.) are available.

A collective review of literature and comparison of approaches ensures an evolution of techniques and improved application of modelling software. Often available literature is not considered prior to design testing, or isolated studies with fitted validation cases are used resulting in incorrectly predicted flow behaviour. This collection and revision of findings serves to provide a “fuller-picture” of commonly applied modelling techniques, shortcomings, and possible solutions.

5 Conclusions

A growing number of researchers and design engineers are using CFD for wake analysis of hydrokinetic turbine design. This is often done without sufficient model validation. Although investigation into simplified analytical models for tidal energy applications has been extensively researched, for inland schemes design spacing may be governed by blockage ratios, confinement, and spatial limitations. Therefore, a more descriptive analysis of the system characteristics and their effects in the complex wake field is necessary. The use of CFD and 3-D modelling of the flow field offers a more in-depth result, which is an advantage over traditional BEM. Here the wake interactions may also be analysed. This paper examines the limitations of commercially available CFD models and methods used in HAHT wake analysis.

Higher order models such as LES and DES are becoming more affordable as computational resources increase in availability. However, a simplified BEM-RANS analysis serves as a lower-cost computational tool which can adequately model the wake dissipation, including effects of retaining structures as well as inlet conditions (e.g., Turbulence). There are however limitations in accurately predicting the near wake, including underestimation of

the TKE present in the flow and a sensitivity to input variables. These limitations must be understood prior to application.

All RANS models and rotor modelling techniques indicated good representations of the turbine performance metrics, which are also often used in literature. However, the performance of these modelling techniques varies when simulating more complex wake dissipation behaviour. Despite the slight inaccuracies, which could be a result of one or more of the mentioned factors, the present study indicates under current available commercial CFD approaches the BEM-CFD approach using RSM-LPS2 model allows a fairly accurate analysis of the near and far wake dissipation rate. The rate of decay of the wake indicated a maximum of 4% difference when the model is analysed using the prescribed conditions without further calibration from validation case discrepancies. The sensitivity of the VD to input parameters and foil properties should be considered and care should be taken to ensure accurate and extensive input data. The model was also shown to be sensitive to turbulent inflow conditions and may therefore be a better tool to employ when analysing flow over a range of operating conditions.

A second validation case with different operational parameters and ambient turbulences showed adequate accuracy in the velocity deficit in the near and far wake. Further, validation cases should investigate the consistency of the BEM-LPS2 solution. However, accuracy and good characterization of uncertainties in experimental results is imperative to proper validation and recommending useful computational modelling methods.

When the full geometry of the turbine is used for analysis, care should be taken in the selection of turbulence models and mesh refinement, specifically in the near wake where small changes in mesh size significantly influence results. This study has highlighted some inaccuracies in wake dissipation rates resulting from the use of full rotor geometry when coupled with the analysed approaches. This may be due to the lack of resolution in the small eddies in the wake, or inaccuracies in the fluid body interaction with the rotating blades. The result is stronger vortices in the near wake and rapidly degrading TKE in the bypass flow which delays wake dissipation. Thus, it may be preferential to use a disk approach rather than the full rotating geometry when employing RANS models.

Although higher fidelity Reynolds Stress models are preferable to accurately model the wake, computational time and expense may not allow this. Solutions to offset the poor performance of eddy viscosity models due to accelerated TKE depletion can be counteracted by limiting the minimum value of TI in the flow field. A few investigations into possible solutions have been examined, and a simple solution may be to specify an ambient turbulent source term in the investigated validation case. However, this solution should be used with care and requires further investigation.

It is known in experimental wake studies and validation cases that scaling parameters and keeping to required uniformity laws are of concern. This is especially true when considering the Reynolds number and the lack of confidence in models validated further from the Reynolds number experienced at full-scale. Although Reynolds number dependence was not relevant here, as no scaling was carried out, numerical models have shown to have strong Reynolds dependencies.

CFD is a useful tool for wake analysis and provides detailed results of the wake structure and dissipation rate when coupled with the correct input parameters and solvers required to simulate the complexities of wake flow. CFD is preferable over simplified numerical tools, e.g., analytical models because it resolves the effects of wake interaction, retaining structures and blockage effects, which can be significant in inland hydrokinetic schemes due to spatial limitations. Hence, it is a useful tool for design and analysis of inland HAHT schemes.

6 Acknowledgements

The work was supported by the University of Pretoria as well as the Technical University of Munich. The computational capabilities were made possible due to academic hours allocated by the Centre for High Performance Computing (CHPC) South Africa. Siemens STAR-CCM+ Simcenter software and support was

provided by Aerotherm Computational Dynamics (Pty) Ltd. Experimental results were obtained from Sandia Laboratories repository. All contributors are thanked for their kind assistance and support.

Funding: The experimental results used in the present study was supported by Sandia National Laboratories. Sandia National Laboratories is a multi-mission laboratory managed and operated by National Technology and Engineering Solutions of Sandia, LLC., a wholly owned subsidiary of Honeywell International, Inc., for the U.S. Department of Energy's National Nuclear Security Administration under contract DE-NA0003525. This paper describes objective technical results and analysis. Any subjective views or opinions that might be expressed in the paper do not necessarily represent the views of the U.S. Department of Energy or the United States Government.

7 References

[1] EPRI, Assessment and Mapping of the Riverine Hydrokinetic Resource in the Continental United States., Palo Alto, CA, 2012.

[2] V.S. Neary, B. Gunawan, D.C. Sale, Turbulent inflow characteristics for hydrokinetic energy conversion in rivers, Renew. Sustain. Energy Rev. 26 (2013) 437–445. https://doi.org/10.1016/j.rser.2013.05.033.

[3] M. Guerra, J. Thomson, Wake measurements from a hydrokinetic river turbine, Renew. Energy. 139 (2019) 483–495. https://doi.org/https://doi.org/10.1016/j.renene.2019.02.052.

[4] A.W. Fontaine, W. Straka, R. Meyer, M. Jonson, V.S. Neary, Performance and wake flow characterization of a 1:8.7 scale reference USDOE MHKF1 hydrokinetic turbine to establish a verification and validation test database, Renew. Energy. (2020).

[5] C.M. Niebuhr, M. van Dijk, V.S. Neary, J.N. Bhagwan, A review of hydrokinetic turbines and enhancement techniques for canal installations: Technology, applicability and potential, Renew. Sustain. Energy Rev. 113 (2019). https://doi.org/10.1016/j.rser.2019.06.047.

[6] C.M. Niebuhr, M. van Dijk, J.N. Bhagwan, Development of a design and implementation process for the integration of hydrokinetic devices into existing infrastructure in South Africa, Water SA. 45 (2019) 434–446.

[7] L.E. Myers, A.S. Bahaj, An experimental investigation simulating flow effects in first generation marine current energy converter arrays, Renew. Energy. 37 (2012) 28–36. https://doi.org/10.1016/j.renene.2011.03.043.

[8] V.S. Neary, B. Gunawan, C. Hill, L.P. Chamorro, Near and far field flow disturbances induced by model hydrokinetic turbine: ADV and ADP comparison, Renew. Energy. 60 (2013) 1–6. https://doi.org/10.1016/j.renene.2013.03.030.

[9] M. De Dominicis, R. O'Hara Murray, J. Wolf, Multi-scale ocean response to a large tidal stream turbine array, Renew. Energy. 114 (2017) 1160–1179. https://doi.org/10.1016/j.renene.2017.07.058.

[10] A.J. Goward Brown, S.P. Neill, M.J. Lewis, Tidal energy extraction in three-dimensional ocean models, Renew. Energy. 114 (2017) 244–257. https://doi.org/10.1016/j.renene.2017.04.032.

[11] C.A. Consul, R.H.J. Willden, S.C. McIntosh, Blockage effects on the hydrodynamic performance of a marine cross-flow turbine, Philos. Trans. R. Soc. A. 371 (2013). https://doi.org/10.1098/rsta.2012.0299.

[12] J. Riglin, F. Carter, N. Oblas, W.C. Schleicher, C. Daskiran, A. Oztekin, Experimental and numerical characterization of a full-scale portable hydrokinetic turbine prototype for river applications, Renew. Energy. 99 (2016) 772–783.

[13] A.S. Bahaj, A.F. Molland, J.R. Chaplin, W.M.J. Batten, Power and thrust measurements of marine current turbines under various hydrodynamic flow conditions in a cavitation tunnel and a towing tank, Renew. Energy. 32 (2007) 407–426. https://doi.org/10.1016/j.renene.2006.01.012.

[14] S. Salunkhe, O. El Fajri, S. Bhushan, D. Thompson, D. O'Doherty, T. O'Doherty, A. Mason-Jones, Validation of tidal stream turbine wake predictions and analysis of wake recovery mechanism, J. Mar. Sci. Eng. 7 (2019). https://doi.org/10.3390/jmse7100362.

[15] D. Olivieri, D. Ingram, Tidal array scale numerical modelling . Interactions within a farm (unsteady Flow)., Edinburgh, 2013.

[16] C. Hill, V.S. Neary, M. Guala, F. Sotiropoulos, Performance and Wake Characterization of a Model Hydrokinetic Turbine: The Reference Model 1 (RM1) Dual Rotor Tidal Energy Converter, in: Energies, 2020: pp. 1–21. https://doi.org/10.3390/en13195145.

[17] N. Kolekar, A. Banerjee, Performance characterization and placement of a marine hydrokinetic turbine in a tidal channel under boundary proximity and blockage effects, Appl. Energy. 148 (2015) 121–133. https://doi.org/10.1016/j.apenergy.2015.03.052.

[18] A.H. Birjandi, E.L. Bibeau, V. Chatoorgoon, A. Kumar, Power measurement of hydrokinetic turbines with free-surface and blockage effect, Ocean Eng. 69 (2013) 9–17. https://doi.org/10.1016/j.oceaneng.2013.05.023.

[19] T.A.A. Adcock, S. Draper, T. Nishino, Tidal power generation – A review of hydrodynamic modelling, J. Power Energy. 0 (2015) 1–17. https://doi.org/10.1177/0957650915570349.
[20] J. Walker, K. Flack, E. Lust, S. MP, L. Luznik, Experimental and numerical studies of blade roughness and fouling on marine current turbine performance, Renew. Energy. 66 (2014) 257–267.
[21] B. Mannion, V. McCormack, S.B. Leen, S. Nash, A CFD investigation of a variable-pitch vertical axis hydrokinetic turbine with incorporated flow acceleration, J. Ocean Eng. Mar. Energy. 5 (2019) 21–39. https://doi.org/10.1007/s40722-019-00130-1.
[22] M.J. Churchfield, Y. Li, P.J. Moriarty, A large eddy simulation study of wake propagation and power production in an array of tidal-current turbines, Philos. Trans. R. Soc. A. 371 (2013) 1–15.
[23] B. Sanderse, S.P. van der Pijl, B. Koren, Review of computational fluid dynamics for wind turbine wake aerodynamics, Wind Energy. 14 (2011) 799–819. https://doi.org/10.1002/we.
[24] P. Mycek, B. Gaurier, G. Germain, G. Pinon, E. Rivoalen, Experimental study of the turbulence intensity effects on marine current turbines behaviour. Part I: One single turbine, Renew. Energy. 66 (2014) 729–746. https://doi.org/10.1016/j.renene.2013.12.048.
[25] F. Maganga, G. Germain, J. King, G. Pinon, E. Rivoalen, Experimental characterisation of flow effects on marine current turbine behaviour and on its wake properties, IET Renew. Power Gener. 4 (2010) 498–509. https://doi.org/10.1049/iet-rpg.2009.0205.
[26] P. Mycek, B. Gaurier, G. Germain, G. Pinon, E. Rivoalen, Experimental study of the turbulence intensity effects on marine current turbines behaviour. Part II: Two interacting turbines, Renew. Energy. 68 (2014) 876–892. https://doi.org/10.1016/j.renene.2013.12.048.
[27] M. Edmunds, R. Malki, A.J. Williams, I. Masters, T.N. Croft, Aspects of tidal stream turbine modelling in the natural environment using a coupled BEM – CFD model, 7 (2014) 20–42.
[28] R. Malki, I. Masters, A.J. Williams, T.N. Croft, Planning tidal stream turbine array layouts using a coupled blade element momentum e computational fluid dynamics model, Renew. Energy. 63 (2014) 46–54.
[29] M.J. Churchfield, Y. Li, P.J. Moriarty, A large-eddy simulation study of wake propagation and power production in an array of tidal-current turbines, Philos. Trans. R. Soc. A. 371 (2013).
[30] Y. Dai, Z. Ren, K. Wang, W. Li, Z. Li, W. Yan, Optimal sizing and arrangement of tidal current farm, IEEE Trans. Sustain. Energy. 9 (2018) 168–177. https://doi.org/10.1109/TSTE.2017.2719042.
[31] M. Kartezhnikova, T.M. Ravens, Hydraulic impacts of hydrokinetic devices, Renew. Energy. 66 (2014) 425–432. https://doi.org/10.1016/j.renene.2013.12.034.
[32] W.H. Lam, L. Chen, Equations used to predict the velocity distribution within a wake from a horizontal-axis tidal-current turbine, Ocean Eng. 79 (2014) 35–42. https://doi.org/10.1016/j.oceaneng.2014.01.005.
[33] P. Pyakurel, J.H. Vanzwieten, T. Wenlong, P. Ananthakrishnan, Analytic Characterization of the Wake Behind In-stream Hydrokinetic Turbines, Mar. Technol. Soc. J. 51 (2017) 58–71.
[34] P.A.S.F. Silva, T.F. De Oliveira, A.C.P. Brasil Junior, J.R.P.P. Vaz, T.F.D.E. Oliveira, A.C.P.B. Junior, J.R.P.P. Vaz, Numerical Study of Wake Characteristics in a Horizontal-Axis Hydrokinetic Turbine, Ann. Braziian Acad. Sci. 88 (2016) 2441–2456. https://doi.org/10.1590/0001-3765201620150652.
[35] M.E. Harrison, W.M.J. Batten, L.E. Myers, A.S. Bahaj, Comparison between CFD simulations and experiments for predicting the far wake of horizontal axis tidal turbines, IET Renew. Power Gener. 4 (2010) 613. https://doi.org/10.1049/iet-rpg.2009.0193.
[36] A.S. Bahaj, L.E. Myers, M.D. Thomson, N. Jorge, Characterising the wake of horizontal axis marine current turbines, 7th Eur. Wave Tidal Energy Conf. (2007).
[37] M. Boudreau, G. Dumas, Comparison of the wake recovery of the axial-flow and cross-flow turbine concepts, J. Wind Eng. Ind. Aerodyn. 165 (2017) 137–152. https://doi.org/10.1016/j.jweia.2017.03.010.
[38] B. Chen, Lin, J. Lin, S. Wang, Experimental study of wake structure behind a horizontal axis tidal stream turbine, Appl. Energy. 196 (2017) 82–96.
[39] P.A.S.F. Silva, T.F. De Oliveira, A.C.P. Brasil Junior, J.R.P. Vaz, Numerical study of wake characteristics in a horizontal-axis hydrokinetic turbine, An. Acad. Bras. Cienc. 88 (2016) 2441–2456. https://doi.org/10.1590/0001-3765201620150652.
[40] L.P. Chamorro, C. Hill, S. Morton, C. Ellis, R.E.A. Arndt, F. Sotiropoulos, On the interaction between a turbulent open channel flow and an axial-flow turbine, J. Fluid Mech. 716 (2013) 658–670. https://doi.org/10.1017/jfm.2012.571.
[41] A.S. Bahaj, L.E. Myers, R.I. Rawlinson-Smith, M. Thomson, The effect of boundary proximity upon the wake structure of horizontal axis marine current turbines, J. Offshore Mech. Arct. Eng. 134 (2011) 1–8. https://doi.org/10.1115/1.4004523.
[42] P. Aghsaee, C.D. Markfort, Effects of flow depth variations on the wake recovery behind a horizontal-axis hydrokinetic in-stream turbine, Renew. Energy. 125 (2018) 620–629. https://doi.org/10.1016/j.renene.2018.02.137.
[43] C. Garrett, P. Cummins, The efficiency of a turbine in a tidal channel, J. Fluid Mech. 588 (2007) 243–

251. https://doi.org/10.1017/S0022112007007781.
[44] A. Olczak, T. Stallard, T. Feng, P.K. Stansby, Comparison of a RANS blade element model for tidal turbine arrays with laboratory scale measurements of wake velocity and rotor thrust, J. Fluids Struct. 64 (2016) 87–106. https://doi.org/10.1016/j.jfluidstructs.2016.04.001.
[45] B. Sanderse, Aerodynamics of wind turbine wakes: Literature review, 2009. https://doi.org/10.1002/we.
[46] M. Edmunds, A.J. Williams, I. Masters, T.N. Croft, An enhanced disk averaged CFD model for the simulation of horizontal axis tidal turbines, 101 (2017) 67–81.
[47] D. Mehta, A.H. Van Zuijlen, B. Koren, J.G. Holierhoek, H. Bijl, Large Eddy Simulation of wind farm aerodynamics : A review, J. Wind Eng. Ind. Aerodyn. 133 (2014) 1–17. https://doi.org/10.1016/j.jweia.2014.07.002.
[48] P.R. Spalart, C.L. Rumsey, Effective inflow conditions for turbulence models in aerodynamic calculations, AIAA J. 45 (2007) 2544–2553. https://doi.org/10.2514/1.29373.
[49] R. Mikkelson, J.N. Sorensen, W.Z. Schen, Modelling and analysis of the flow field around a coned rotor, Wind Energy. 4 (2001) 121–135.
[50] O. a Lo Brutto, V.T. Nguyen, S.S. Guillou, H. Gualous, B. Boudart, Reanalyse of an Analytical Model for One Tidal Turbine Wake Prediction, in: Proc. 11th Eur. Wave Tidal Energy Conf., Nantes, France, 2015.
[51] W.H. Lam, L. Chen, R. Hashim, Analytical wake model of tidal current turbine, Energy. 79 (2015) 512–521. https://doi.org/10.1016/j.energy.2014.11.047.
[52] L. Tian, W. Zhu, W. Shen, N. Zhao, Z. Shen, Development and validation of a new two-dimensional wake model for wind turbine wakes, J. Wind Eng. Ind. Aerodyn. 137 (2015) 90–99. https://doi.org/10.1016/j.jweia.2014.12.001.
[53] T. Nishino, R.H.J. Willden, Effects of 3-D channel blockage and turbulent wake mixing on the limit of power extraction by tidal turbines, Int. J. Heat Fluid Flow. 37 (2012) 123–135. https://doi.org/10.1016/j.ijheatfluidflow.2012.05.002.
[54] T. Nishino, R.H.J. Willden, Two-scale dynamics of flow past a partial cross-stream array of tidal turbines, (2013) 220–244. https://doi.org/10.1017/jfm.2013.340.
[55] C. Gotelli, M. Musa, M. Guala, C. Escauriaza, Experimental and Numerical Investigation of Wake Interactions of Marine Hydrokinetic Turbines, Energies. 12 (2019) 1–17. https://doi.org/10.3390/en12163188.
[56] J. Whale, C.G. Anderson, R. Bareiss, S. Wagner, An experimental and numerical study of the vortex structure in the wake of a wind turbine, J. Wind Eng. Ind. Aerodyn. 84 (2000) 1–21. https://doi.org/10.1016/S0167-6105(98)00201-3.
[57] G. Pinon, P. Mycek, G. Germain, E. Rivoalen, Numerical simulation of the wake of marine current turbines with a particle method, Renew. Energy. 46 (2012) 111–126. https://doi.org/10.1016/j.renene.2012.03.037.
[58] M. Fabrice, P. Gregory, G. Gregory, R. Elie, Numerical simulation of the wake of marine current turbines with a particle method, in: World Renew. Energy Congr. X, Glasgow, 2008.
[59] W. Tian, Z. Mao, H. Ding, Design, test and numerical simulation of a low-speed horizontal axis hydrokinetic turbine, Int. J. Nav. Archit. Ocean Eng. 10 (2018) 782–793.
[60] M. Ge, Y. Wu, Y. Liu, X.I.A. Yang, A two-dimensional Jensen model with a Gaussian-shaped velocity deficit, Renew. Energy. 141 (2019) 46–56. https://doi.org/10.1016/j.renene.2019.03.127.
[61] P. Pyakurel, W. Tian, J.H. VanZwieten, M. Dhanak, Characterization of the mean flow field in the far wake region behind ocean current turbines, J. Ocean Eng. Mar. Energy. 3 (2017) 113–123. https://doi.org/10.1007/s40722-017-0075-9.
[62] L.. Contreras, Y. Lopez, S. Lain, CFD Simulation of a Horizontal Axis Hydrokinetic Turbine, Renew. Energy Power Qual. J. 1 (2017) 512–517. https://doi.org/10.24084/repqj15.376.
[63] M. Shives, C. Crawford, Turbulence Modelling for Accurate Wake Prediction in Tidal Turbine Arrays, in: 5th Int. Conf. Ocean Energy, Halifax, Canada, 2014.
[64] F.R. Menter, Turbulence Modeling for Engineering Flows, 2011. http://cfd.spbstu.ru/agarbaruk/c/document_library/DLFE-41517.pdf.
[65] J. McNaughton, S. Rolfo, D.D. Apsley, I. Afgan, P.K. Stansby, T. Stallard, CFD prediction of turbulent flow on an experimental tidal stream turbine using RANS modelling, 1st Asian Wave Tidal Conf. Ser. (2012). https://doi.org/10.1017/CBO9781107415324.004.
[66] S. Kang, I. Borazjani, J.A. Colby, F. Sotiropoulos, Numerical simulation of 3D flow past a real-life marine hydrokinetic turbine, Adv. Water Resour. 39 (2012) 33–43. https://doi.org/10.1016/j.advwatres.2011.12.012.
[67] P.R. Spalart, Strategies for Turbulence Modeling and Simulations, Int. J. Heat Fluid Flow. 21 (2000) 252–263.
[68] T. Blackmore, W.M.J. Batten, A.S. Bahaj, Influence of turbulence on the wake of a marine current

turbine simulator, Proc. R. Soc. A Math. Phys. Eng. Sci. 470 (2014) 1–17. https://doi.org/10.1098/rspa.2014.0331.
[69] S. Kang, X. Yang, F. Sotiropoulos, On the onset of wake meandering for an axial flow turbine in a turbulent open channel flow, J. Fluid Mech. 744 (2014) 376–403. https://doi.org/10.1017/jfm.2014.82.
[70] G. Bai, J. Li, P. Fan, G. Li, Numerical investigations of the effects of different arrays on power extractions of horizontal axis tidal current turbines, Renew. Energy. 53 (2013) 180–186. https://doi.org/10.1016/j.renene.2012.10.048.
[71] S. Lain, L.T. Contreras, O. Lopez, A review on computational fluid dynamics modeling and simulation of horizontal axis hydrokinetic turbines, J. Brazilian Soc. Mech. Sci. Eng. (2019). https://doi.org/10.1007/s40430-019-1877-6.
[72] L.J. Vermeer, J.N. Sørensen, A. Crespo, Wind turbine wake aerodynamics, Prog. Aerosp. Sci. 39 (2003) 467–510. https://doi.org/10.1016/S0376-0421(03)00078-2.
[73] I. Masters, A. Williams, T.N. Croft, M. Togneri, M. Edmunds, E. Zangiabadi, I. Fairley, H. Karunarathna, A comparison of numerical modelling techniques for tidal stream turbine analysis, Energies. 8 (2015) 7833–7853. https://doi.org/10.3390/en8087833.
[74] Y. El khchine, M. Sriti, Tip Loss Factor Effects on Aerodynamic Performances of Horizontal Axis Wind Turbine, in: 2nd Int. Conf. Adv. Clean Energy Res., Berlin, Germany, 2017: pp. 2–6.
[75] W.Z. Shen, R. Mikkelsen, J.N. Sorensen, Tip loss corrections for wind turbine Computations, Wind Energy. 8 (2005) 457–475. https://doi.org/10.1002/we.153.
[76] I. Masters, J.C. Chapman, M.R. Willis, J.A.C. Orme, A robust blade element momentum theory model for tidal stream turbines including tip and hub loss corrections, J. Mar. Eng. Technol. 10 (2014) 25–35. https://doi.org/10.1080/20464177.2011.11020241.
[77] T. Burton, N. Jenkins, D. Sharpe, E. Bossanyi, Wind Energy Handbook (2nd Edition), 2nd ed., John Wiley & Sons, 2011. https://doi.org/10.1007/978-3-540-88258-9-1.
[78] Q. Guo, L. Zhou, Z. Wang, Comparison of BEM-CFD and full rotor geometry simulations for the performance and flow field of a marine current turbine, Renew. Energy. 75 (2015) 640–648.
[79] R. Malki, A.J. Williams, T.N. Croft, M. Togneri, I. Masters, A coupled blade element momentum – Computational fluid dynamics model for evaluating tidal stream turbine performance, Appl. Math. Model. 37 (2013) 3006–3020. https://doi.org/10.1016/j.apm.2012.07.025.
[80] S.R. Turnock, A.B. Phillips, J. Banks, R. Nicholls-Lee, Modelling tidal current turbine wakes using a coupled RANS-BEMT approach as a tool for analysing power capture of arrays of turbines, Ocean Eng. 38 (2011) 1300–1307. https://doi.org/10.1016/j.oceaneng.2011.05.018.
[81] R. Malki, I. Masters, A.J. Williams, N. Croft, The variation in wake structure of a tidal stream turbine with flow velocity, in: Int. Conf. Comput. Methods Mar. Eng., Barcelona, 2011. https://doi.org/10.1007/978-94-007-6143-8.
[82] I. Masters, R. Malki, A.J. Williams, T.N. Croft, The influence of flow acceleration on tidal stream turbine wake dynamics : A numerical study using a coupled BEM – CFD model, Appl. Math. Model. 37 (2013) 7905–7918. https://doi.org/10.1016/j.apm.2013.06.004.
[83] D. Gajardo, C. Escauriaza, D.M. Ingram, Capturing the development and interactions of wakes in tidal turbine arrays using a coupled BEM-DES model, Ocean Eng. 181 (2019) 71–88. https://doi.org/10.1016/j.oceaneng.2019.03.064.
[84] L. Myers, A.S. Bahaj, Near wake properties of horizontal axis marine current turbines, in: Eighth Eur. Wave Tidal Energy Cnference, Uppsala, Swedeb, 2009: pp. 558–565.
[85] M.H.B. Ahmadi, Influence of upstream turbulence on the wake characteristics of a tidal stream turbine, Renew. Energy. 132 (2019) 989–997. https://doi.org/10.1016/j.renene.2018.08.055.
[86] C.E. Morris, D.M. O'Doherty, A. Mason-Jones, T. O'Doherty, Evaluation of the swirl characteristics of a tidal stream turbine wake, Int. J. Mar. Energy. 14 (2016) 198–214. https://doi.org/10.1016/j.ijome.2015.08.001.
[87] M.S. Siddiqui, A.. di. Rasheed, T. Kvamsdal, M. Tabib, Influence of Tip Speed Ratio on Wake Flow Characteristics Utilizing Fully Resolved CFD Methodology, J. Phys. Conf. Ser. 854 (2017). https://doi.org/10.1088/1742-6596/854/1/012043.
[88] I. Nezu, H. Nakagawa, G.H. Jirka, Turbulence in Open-Channel flows, J. Hydraul. Eng. 120 (1994).
[89] V.S. Neary, B. Gunawan, C. Hill, L.P. Chamorro, Near and far field flow disturbances induced by model hydrokinetic turbine: ADV and ADP comparison, Renew. Energy. 60 (2013) 1–6. https://doi.org/10.1016/j.renene.2013.03.030.
[90] J.I. Whelan, J.M.R. Graham, J. Peiró, A free-surface and blockage correction for tidal turbines, J. Fluid Mech. 624 (2009) 281–291. https://doi.org/10.1017/S0022112009005916.
[91] L.E. Myers, A.S. Bahaj, Experimental analysis of the flow field around horizontal axis tidal turbines by use of scale mesh disk rotor simulators, Ocean Eng. 37 (2010) 218–227. https://doi.org/10.1016/j.oceaneng.2009.11.004.

[92] O. El Fajri, S. Bhushan, D.S. Thompson, T. O'Doherty, Numerical investigation of shallow-water effects on hydrokinetic turbine wake recovery, Int. Mar. Energy J. 3 (2020) 25–35. https://doi.org/10.36688/imej.3.25-35.
[93] T. Stallard, R. Collings, T. Feng, J. Whelan, Interactions between tidal turbine wakes: Experimental study of a group of three-bladed rotors, Philos. Trans. R. Soc. A Math. Phys. Eng. Sci. 371 (2013). https://doi.org/10.1098/rsta.2012.0159.
[94] P. Bachant, M. Wosnik, Reynolds Number Dependence of Cross-Flow Turbine Performance and Near-Wake Characteristics, in: Proc. 2nd Mar. Energy Technol. Symp., Seattle, WA, 2014.
[95] H. Ross, B. Polagye, An experimental assessment of analytical blockage corrections for turbines, Renew. Energy. 152 (2020) 1328–1341.
[96] C. Hill, V.S. Neary, U. S. Department of Energy Reference Model Program RM1 : Experimental Results, Sandia Natl. Lab. (2014).
[97] B. Gunawan, V.S. Neary, J.R. McNutt, ORNL ADV Post-Processing Guide and MATLAB Algorithms for MHK Site Flow and Turbulence Analysis, US Department of Energy, Oak Ridge, Tennessee, 2011.
[98] M.H. Nasef, W.A. El-Askary, A.A. AbdEL-hamid, H.E. Gad, Evaluation of Savonius rotor performance: Static and dynamic studies, J. Wind Eng. Ind. Aerodyn. 123 (2013) 1–11. https://doi.org/10.1016/j.jweia.2013.09.009.
[99] J. Franke, C. Hirsch, A.G. Jensen, H.W. Krus, P.S. Schatzmann, S.D. Miles, J.A. Wisse, N.G. Wright, Recommendations on the use of CFD in wind engineering, COST Action C14 Impact Wind Storm City Life Urban Environ. (2004).
[100] V.B. Miller, L.A. Schaefer, Dynamic modeling of hydrokinetic energy extraction, J. Fluids Eng. Trans. ASME. 132 (2010) 1–7. https://doi.org/10.1115/1.4002431.
[101] C. Daskiran, J. Riglin, W. Schleicher, A. Oztekin, Transient analysis of micro-hydrokinetic turbines for river applications, 129 (2017) 291–300.
[102] I. Afgan, J. Mcnaughton, S. Rolfo, D.D. Apsley, T. Stallard, P. Stansby, Turbulent flow and loading on a tidal stream turbine by LES and RANS, Int. J. Heat Fluid Flow. 43 (2013) 96–108. https://doi.org/10.1016/j.ijheatfluidflow.2013.03.010.
[103] F.R. Menter, Two-equation eddy-viscosity turbulence models for engineering applications, AIAA J. 32 (1994) 1598–1605.
[104] F.R. Menter, M. Kuntz, R. Langtry, Ten years of industrial experience with the SST turbulence model, Turbul Heat Mass Transf. 4 (2003) 625–632.
[105] C.G. Speziale, S. Sarkar, T.B. Gatski, Modelling the pressure-strain correlation of turbulence : An invariant dynamical systems approach, J. Fluid Mech. 227 (1991) 245–272. https://doi.org/10.1017/S0022112091000101.
[106] S. Sarkar, B. Lakshmanan, Application of a Reynolds stress turbulence model to the compressible shear layer, AIAA J. 29 (1991) 743–749. https://doi.org/10.2514/3.10649.
[107] P.J. Roache, Perspectvie: A method for Uniform Reporting of Grid Refinement Studies, J. Fluids Eng. Trans. ASME. 116 (1994) 405–413.
[108] M.M. Gibson, B.E. Launder, Ground effects on pressure fluctuations in the atmospheric boundary layer, J. Fluid Mech. 86 (1978) 491–511. https://doi.org/10.1017/S0022112078001251.
[109] M. Allmark, R. Ellis, C. Lloyd, S. Ordonez-Sanchez, K. Johannesen, C. Byrne, C. Johnstone, T. O'Doherty, A. Mason-Jones, The development, design and characterisation of a scale model Horizontal Axis Tidal Turbine for dynamic load quantification, Renew. Energy. 156 (2020) 913–930. https://doi.org/10.1016/j.renene.2020.04.060.
[110] L. Lavaroni, S.J. Watson, M.J. Cook, M.R. Dubal, A comparison of actuator disc and BEM models in CFD simulations for the prediction of offshore wake losses, J. Phys. Conf. Ser. 524 (2014). https://doi.org/10.1088/1742-6596/524/1/012148.
[111] C. Hill, V.S. Neary, B. Gunawan, M. Guala, F. Sotiropoulos, U. S. Department of Energy Reference Model Program RM1 : Experimental Results, Minneapolis, 2014.
[112] M.J. Hoffmann, R. Reuss Ramsay, G.M. Gregorek, Effects of grit roughness and pitch oscillations on the NACA 4415 airfoil, 1996. https://doi.org/10.2172/266691.
[113] O.M. Fouatih, B. Imine, M. Medale, Numerical/experimental investigations on reducing drag penalty of passive vortex generators on a NACA 4415 airfoil, Wind Energy. 22 (2019) 1003–1017. https://doi.org/10.1002/we.2330.
[114] S. Wallin, A. V. Johansson, An explicit algebraic Reynolds stress model for incompressible and compressible turbulent flows, J. Fluid Mech. 403 (2000) 89–132. https://doi.org/10.1017/S0022112099007004.
[115] D. McBride, T.N. Croft, M. Cross, A coupled finite volume method for the computational modelling of mould filling in very complex geometries, Comput. Fluids. 37 (2008) 170–180.